Cerebral Cortex March 2009;19:624-639
doi:10.1093/cercor/bhn116
Advance Access publication July 18, 2008

Functional Imaging of the Parietal Cortex during Action Execution and Observation

Mina N. Evangeliou[1], Vassilis Raos[1], Claudio Galletti[2] and Helen E. Savaki[1]

[1]Department of Basic Sciences, Faculty of Medicine, School of Health Sciences, University of Crete and Institute of Applied and Computational Mathematics, Foundation for Research and Technology, Hellas, Greece and [2]Dipartimento di Fisiologia Umana e Generale, Università di Bologna, Bologna, Italy

We used the ^{14}C-deoxyglucose method to map the functional activity in the cortex of the lateral and medial parietal convexity, the intraparietal and the parietoccipital sulci of monkeys which either reached and grasped a 3D-object or observed the same reaching-to-grasp movements executed by a human. Execution of reaching-to-grasp induced activations in the superior parietal areas SI-forelimb/convexity, PE, PE caudal (PEc); in the intraparietal areas PE intraparietal (PEip), medial intraparietal (MIP), 5 intraparietal posterior, ventral intraparietal (VIP), anterior intraparietal (AIP), lateral intraparietal dorsal; in the inferior parietal areas PF, PFG, PG; in the parietoccipital areas V6, V6A-dorsal; in the medial cortical areas PGm/7m and retrosplenial cortex. Observation of reaching-to-grasp activated areas SI-forelimb/convexity, PE lateral, PEc, PEip, MIP, VIP, AIP, PF, V6, PGm/7m, 31, and retrosplenial cortex. The common activations were stronger for execution than for observation and the interhemispheric differences were smaller for observation than for execution, contributing to the attribution of action to the correct agent. The extensive overlap of parietal networks activated for action execution and observation supports the "mental simulation theory" which assigns the role of understanding others' actions to the entire distributed neural network responsible for the execution of actions, and not the concept of "mirroring" which reflects the function of a certain class of cells in a couple of cortical areas.

Keywords: action observation, grasping, intraparietal cortex, mental simulation, parietal lobule, parietoccipital cortex

Introduction

Attributing actions to the correct agent and assigning meaning to the actions of other subjects is an essential aspect of efficient behavior. This underlines the importance of examining whether the production and perception of actions rely on different or common distributed neural systems. It was recently shown that the neural system that helps match action perception to action generation encompasses widespread frontal and cingulate cortical circuits. We demonstrated that extensive regions of both the lateral- and medial-frontal cortex, including several premotor and cingulate areas as well as the primary motor and somatosensory cortices are activated when subjects observe object-related hand actions, and they are activated somatotopically as they are for execution of the same actions (Raos et al. 2004, 2007).

Because the parietal cortex is considered a bridge between perception and action, with neurons in the superior (SPL, mainly Brodmann's area 5) and inferior parietal lobule (IPL, area 7) involved in higher order sensorimotor integration during hand manipulation tasks (Mountcastle et al. 1975), receiving convergent input from different sensory modalities as well as efference copy signals from motor areas to guide eye and forelimb movements (Andersen 1989; Kalaska et al. 1990; Savaki et al. 1993; Colby and Goldberg 1999), we decided to explore whether parietal areas are also involved in the so called "action observation/action execution matching system." We used the [^{14}C]-deoxyglucose (^{14}C-DG) quantitative autoradiographic method (Sokoloff et al. 1977) to obtain high-resolution functional images of the monkey parietal cortical areas activated for execution and observation of reaching-to-grasp. The ^{14}C-DG method is the only imaging approach to offer the following advantages: 1) direct assessment of brain activity, 2) quantitative measurement of glucose consumption, 3) resolution of 20 μm, and 4) cytoarchitectonic identification of cortical areas in sections adjacent to the autoradiographic ones.

We examined 1) the parietal convexity including the superior parietal areas SI, PE, PE caudal (PEc) and the inferior parietal areas PF, PFG, PG, and Opt (Pandya and Seltzer 1982; Gregoriou et al. 2006), 2) the intraparietal cortex including areas, PE intraparietal (PEip), medial intraparietal (MIP), 5 ventral intraparietal (5VIP) (Colby et al. 1988; Matelli et al. 1998; Gregoriou and Savaki 2001) and the caudalmost intraparietal region of the medial bank (5IPp) as well as areas anterior intraparietal (AIP), lateral intraparietal (LIP), lateral occipito-parietal/caudal intraparietal (LOP/CIP), 7VIP of the lateral bank (Colby et al. 1993; Lewis and Van Essen, 2000b; Gregoriou and Savaki, 2001; Tsutsui et al. 2003; Borra et al. 2008), and 3) the medial parietoccipital cortical areas V6A, V6 (Galletti, Fattori, Gamberini, et al. 1999; Galletti, Fattori, Kutz, et al. 1999). Finally, we examined additional medial cortical regions such as the PGm/7m (Pandya and Seltzer 1982; Cavada and Goldman-Rakic 1989a) and the retrosplenial cortical areas 29 and 30 (Morris et al. 1999) as well as area 31 located at the medial surface between the posterior cingulate area 23c and the medial parietal area PGm/7m (Morecraft et al. 2004). Histological examination of the brain sections enabled us to assign most of the activated regions of the reconstructed metabolic maps to cytoarchitectonically defined areas of the parietal lobe.

As we demonstrated earlier for the frontal lobe (Raos et al. 2004, 2007), here we show also for the parietal lobe that largely overlapping widespread cortical circuits are recruited for both action perception and action generation. Thus, far from being restricted to the medial and lateral frontal cortical areas, the action observation/execution matching system also involves extensive regions of the lateral, medial and intraparietal cortex of the primate brain. The present findings provide further support to our earlier suggestion that we understand the actions of others by recruiting the same cortical circuits which are responsible for

execution of the same actions, in other words that we understand others' actions by mentally simulating them (Raos et al. 2007).

Methods

Subjects

Six adult female monkeys (*Macaca mulatta*) weighing between 4 and 5 kg were used. Experiments were approved by the institutional animal use committee in accordance with European Council Directive 86/609/EEC. A detailed description of the surgical procedures, the behavioral apparatus and the tasks, the electromyographic (EMG) recording and the eye-position recording was previously reported (Raos et al. 2004). In brief, monkeys had their heads fixed and a water delivery tube attached close to their mouth. For immobilization of the head, a metal bolt was surgically implanted on the head of each monkey with the use of mandibular plates that were secured on the bone by titanium screws (Synthes, Bettlach, Switzerland). All surgical procedures were performed under general anesthesia using aseptic techniques. Digitized electromyograms, recorded from the biceps and wrist extensor muscles with surface electrodes, were previously reported (Raos et al. 2004). Eye movements were recorded with an infrared oculometer (Fig. 1). All monkeys were trained to perform their tasks continuously for at least 1 h/day for several months before the ^{14}C-DG experiment, receiving water as reward. On the day of the ^{14}C-DG experiment, monkeys performed their tasks during the entire experimental period of 45 min.

Behavioral Tasks

The behavioral apparatus was placed in front of the monkeys at shoulder height, 20 or 50 cm away depending on whether the monkey or the experimenter had to reach and grasp. A sliding window (circular window of 8° diameter) at the front side of the apparatus allowed the subject (monkey or experimenter) to grasp a horizontally oriented ring using a digging out grip with the index finger inserted into it (with pronated hand). In order to control for possible rate-related effects, the mean rate of movements was set to be similar for the execution and the observation tasks, as well as for the arm-motion control.

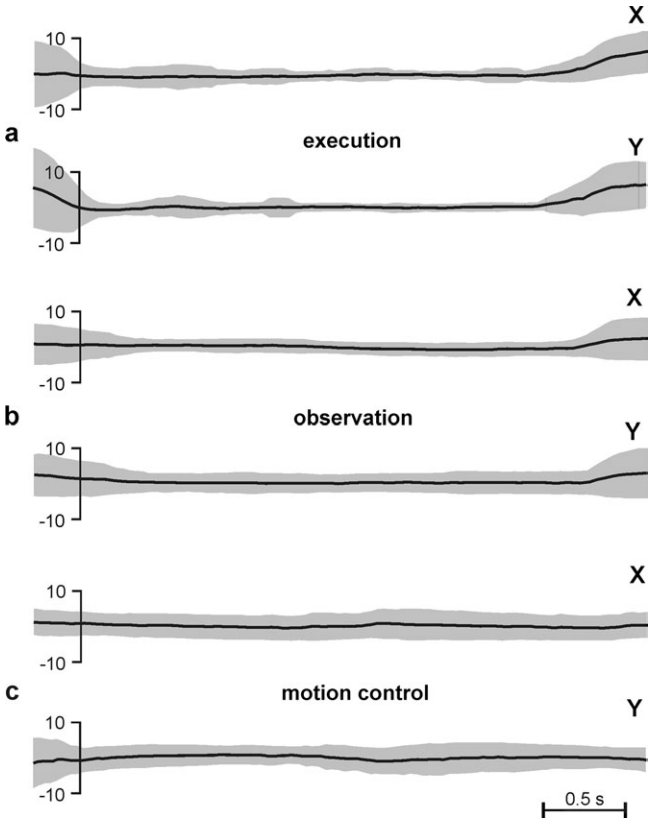

Figure 1. Instantaneous eye-position as a function of time. Solid lines of plots correspond to the instantaneous eye-position averaged over all trials during the critical 10 first min of the ^{14}C-DG experiment. Shaded area around solid lines represents the standard deviation. Eye-position calibration bars (ranging between −10° and +10°) are aligned on the onset of trials. (*a*) Action execution: average of 2 monkeys. (*b*) Action observation: average of 3 monkeys, and (*c*), biological motion control.

Two grasping-execution (E) monkeys were trained to reach and grasp with their left forelimbs, whereas the right ones were restricted. These monkeys were required to fixate the illuminated object behind the opened window for 0.7–1 s, until a dimming of the light would signal reaching, grasping and pulling the ring with the left forelimb while maintaining fixation. The maximum latency to grasp the object was set to 1 s, although the movement was usually completed within 500–600 ms. The E monkeys were allowed to move their eyes outside the window only during the intertrial intervals, which ranged between 2 and 2.5 s.

Three grasping-observation (O) monkeys were first trained to perform the task of the E monkeys, and then trained to observe the same reaching-to-grasp movements executed by the experimenter. Although execution-training took place months before the ^{14}C-DG experiment, in order to cancel any possible interhemispheric effects due to this earlier training, the first monkey was trained to reach and grasp with its left hand, the second one with its right hand and the third one with both hands consecutively. Thus in the observing monkeys, any interhemispheric effect due to the earlier grasping-training would be canceled out by comparing the average quantitative map of the 3 left hemispheres with the average map of the 3 right hemispheres. Both forelimbs of the O monkeys were restricted during the observation-training and during the ^{14}C-DG experiment. The experimenter was always standing on the right side of the monkey and was using the right arm/hand for reaching/grasping. Both reaching and grasping components of the movement were visible to the monkey. Object and movement parameters as well as eye movements and intertrial intervals were similar to the ones described for the E monkeys.

The arm-motion control (Cm) monkey had both hands restricted and was trained to maintain its gaze straight ahead (within the 8° diameter circular window) during the opening of the window of the apparatus, the presentation of the illuminated object behind the opened window, the closure of the window, and while the experimenter was reaching with extended hand toward the closed window (for a total period of 2.7–3 s per trial). The direction of motion and velocity of the experimenter's arm were the same as in the observation task, but the Cm monkey was not exposed to the view of hand preshaping and object-hand interaction. Accordingly, this control monkey was used to take into account the effects of 1) the biological motion of the purposeless (non-goal–directed) reaching arm and 2) the visual stimulation by the 3D object. Therefore, subtraction of the Cm activity from that of the reaching and grasping monkeys revealed the effects of the goal-directed reaching-to-grasp behavioral component. The Cm monkey was allowed to move its eyes outside the circular window only during the intertrial intervals, which ranged between 2 and 2.5 s.

^{14}C-DG Experiments

During the day of the ^{14}C-DG experiment, monkeys were subjected to femoral vein and artery catheterization under general anesthesia, and were allowed 4–5 h to recover. Plasma glucose levels, blood pressure, hematocrit, and blood gases ranged within normal values in all monkeys and remained constant throughout the ^{14}C-DG experiment. A pulse of 100 μCi/kg of 2-deoxy-D-[1-^{14}C] glucose (specific activity 55 mCi/mmol, ARC) dissolved in saline was delivered (by intravenous injection) 5 min after each monkey started its behavioral task. Arterial samples were collected from the catheterized femoral artery during the succeeding 45 min, and the plasma ^{14}C-DG and glucose concentrations were measured. At 45 min, the monkey was sacrificed by intravenous injections of 50 mg sodium thiopental in 5 ml of saline, and then a saturated potassium chloride solution. The cerebral hemispheres, the cerebellum and the spinal cord were removed, frozen in isopentane at –50 °C and stored at –80 °C. Serial 20-μm-thick horizontal sections were cut in a cryostat at –20 °C. Autoradiographs were prepared by exposing these sections, together with precalibrated ^{14}C-standards, with medical X-ray film (Kodak Biomax MR, Paris, France) in X-ray cassettes.

One section every 500 μm was stained with thionine for identification of the cytoarchitectonic borders of cortical areas of the parietal convexity (Pandya and Seltzer 1982; Gregoriou et al. 2006), the IPs (Medalla and Barbas 2006), and the parietoccipital sulcus (POs) (Luppino et al. 2005). Labeling of cortical areas of interest was based on their position relative to surface brain landmarks and their cytoarchitectonically identified borders. Quantitative densitometric analysis of autoradiographs was performed with a computerized image processing system (Imaging Research, Ontario, Canada), which allowed integration of the local cerebral glucose utilization (LCGU) values within each area of interest. LCGU values (in μmol/100 g/min) were calculated as in the authors' previous experiments (Savaki et al. 1993; Raos et al. 2004), from the appropriate kinetic constants for the monkey (Kennedy et al. 1978), by the original operational equation of the ^{14}C-DG method (Sokoloff et al. 1977). Normalization of LCGU values was based on the averaged unaffected gray matter value pooled across all monkeys (Savaki et al. 1993; Gregoriou and Savaki 2003).

Reconstruction of Two-Dimensional Maps of Activity

Two-dimensional (2D) reconstructions of the spatial distribution of metabolic activity within the rostrocaudal and the dorsoventral extent of the cortical areas of the parietal lobe in each hemisphere were generated as previously described (Dalezios et al. 1996; Savaki et al. 1997). To cover the full extent of the cortex of the parietal convexity about 1000 serial horizontal sections, 20 μm thick, were used from each hemisphere of each monkey, whereas 500 sections were used for the reconstruction of the intraparietal cortex, and 650 for the reconstruction of the parietoccipital and the medial parietal cortex. For each horizontal section, a data array was obtained by sampling the LCGU values along a rostrocaudal line parallel to the surface of the cortex and covering all cortical layers (anteroposterior sampling spatial resolution 50 μm/pixel). Every 5 adjacent horizontal sections of 20 μm, data arrays were averaged and plotted to produce one line in the 2D-maps of activity (spatial resolution of plots 100 μm). The posterior crown of the central sulcus (Cs) was used for the alignment of adjacent data arrays in the reconstruction of the parietal convexity. The caudalmost part of the IPs, that is, the intersection of the IPs with the POs and the lunate sulcus (Ls) was used for the alignment of adjacent data arrays in the reconstruction of the IPs. Finally, the intersection of the anterior bank of the POs with the medial surface of the cortical hemisphere (i.e., the medial crown of POs) was used for the alignment of adjacent data arrays in the reconstruction of the POs. Tick marks in each horizontal section labeling surface landmarks of the brain, such as crown, fundus and intersections of sulci, as well as cytoarchitectonically identified borders of cortical areas of interest were used to match the 2D-maps obtained from different hemispheres and animals (see geometrical normalization of maps, below).

Geometrical Normalization of the 2D Maps of Activity

In order to allow for the direct comparison of the sites of activation despite the inter- and intrahemispheric variability, the individual functional (^{14}C-DG) and anatomical (cytoarchitectonic) 2D-maps were further processed to match a reference map. The general procedure of the geometrical normalization of these maps was previously described (Bakola et al. 2006; Raos et al. 2007). In specific, for the parietal-convexity maps (Fig. 2*a*,*b*), the section by section rostrocaudal distances between 1) the posterior crown of the Cs (point of alignment) and the surface landmarks (anterior crown, fundus, posterior crown) of the postcentral dimple (pcd) (for dorsal sections) or the IPs (for middle sections) or the lateral fissure (for ventral sections), 2) the latter and the posterior tip of the brain (for dorsal sections) or the anterior crown of either the superior temporal sulcus or the lateral fissure (for middle sections) were measured. Moreover, the section by section dorsoventral distances between 1) the dorsalmost tip of the brain and the IPs, 2) the latter and the cytoarchitectonically identified Opt/PG border, 3) the latter and the cytoarchitectonic border between PG and PFG, 4) the latter and the PFG/PF border, 5) the latter and the ventral PF border, 6) the latter and the ventralmost section of the reconstruction were also measured. The average of each one of these measures was computed to produce a reference map of landmarks (Fig. 2*b*). The reference map of landmarks in the intraparietal cortex was generated similarly (Fig. 3*a*,*b*). The distances used here were those between the anterior crown

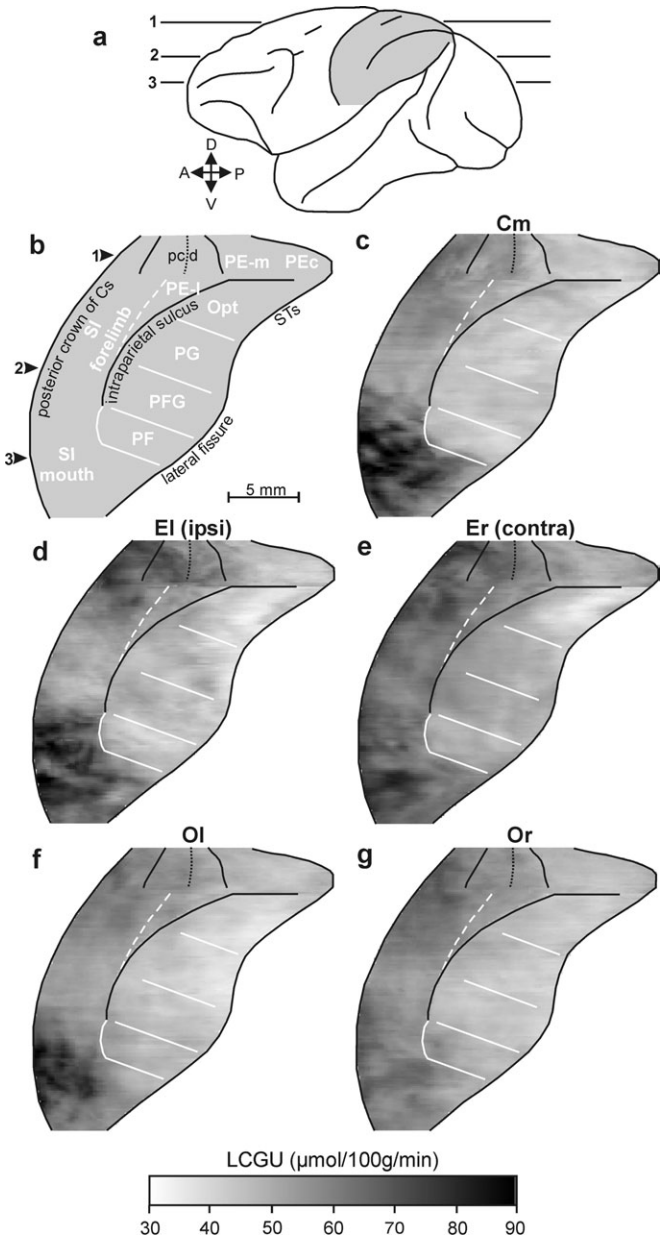

Figure 2. Quantitative 2D-maps of metabolic activity in the lateral parietal cortex. (*a*) Lateral view of the left hemisphere of a monkey brain. Shaded area indicates the reconstructed cortex around the intraparietal sulcus (IPs), surrounded by the central (Cs) and superior temporal (STs) sulci and the lateral fissure. Horizontal lines 1–3 correspond to 3 different dorsoventral levels of brain sectioning. A, anterior; D, dorsal; P, posterior; V, ventral. (*b*) Schematic representation of the geometrically normalized reconstructed cortical field. Black lines correspond to surface landmarks, solid white lines to cytoarchitectonically identified borders of the labeled cortical areas, and the interrupted white line to the SI/PE border based on reported maps. Arrows 1–3 indicate the dorsoventral levels of the corresponding lines in panel a. pcd, postcentral dimple unfolded, with the dotted line representing its fundus and the solid lines its crowns. PE-l, PE-m, lateral and medial portions of area PE. The rest of abbreviated cortical areas are described in the text. (*c*) Averaged map from the 2 hemispheres of the motion-control monkey, Cm. (*d*) Averaged map from the left hemispheres of the 2 action execution monkeys, EI (ipsi). (*e*) Averaged map from the right hemispheres (contralateral to the moving forelimb) of the 2 action execution monkeys, Er (contra). (*f*) Averaged map from the left hemispheres of the 3 action observation monkeys, OI. (*g*) Averaged map from the right hemispheres of the 3 action observation monkeys, Or. Gray-scale bar indicates LCGU values in μmol/100 g/min.

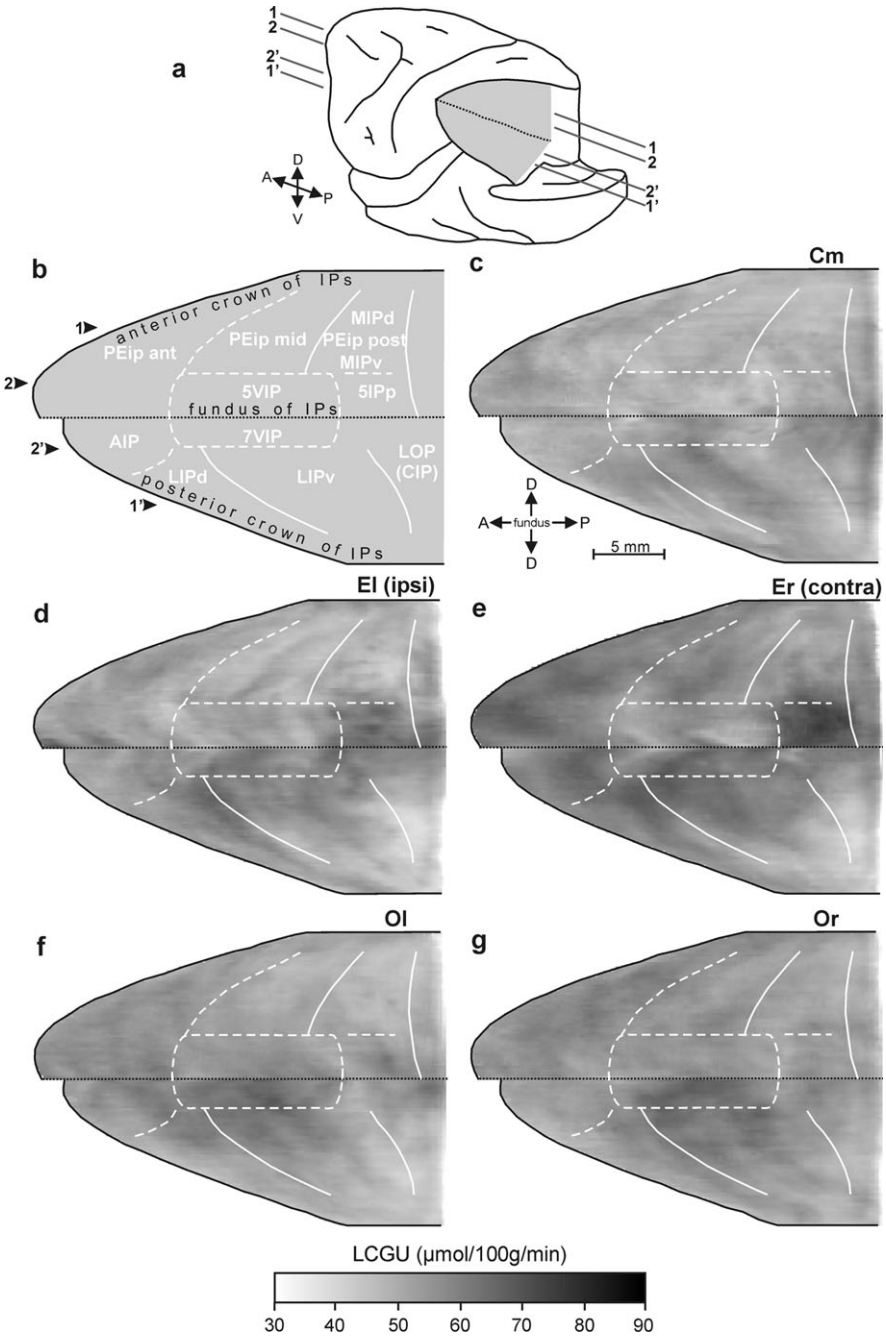

Figure 3. Quantitative 2D-maps of metabolic activity in the intraparietal sulcus (IPs). (*a*) Postero-lateral view of the partially dissected left hemisphere of a monkey brain. The IPL was cut away at the level of the posterior crown of the IPs, the occipital lobe was also cut away at the level of the fundus of POs and Ls, and the IPs was unfolded. Dotted black line depicts the fundus of the sulcus. Shaded area represents the reconstructed medial (upper) and lateral (lower) banks of the cortex. (*b*) Schematic illustration of the geometrically normalized reconstructed cortical field. Black lines correspond to surface landmarks, solid and interrupted white lines correspond to cytoarchitectonically and functionally identified borders, respectively, of the labeled cortical areas. (*c*) Averaged map from the 2 hemispheres of the Cm monkey, Cm. (*d*) Averaged map from the left hemispheres of the 2 execution monkeys, El (ipsi). (*e*) Averaged map from the right hemispheres (contralateral to the moving forelimb) of the same monkeys, Er (contra). (*f*) Averaged map from the left hemispheres of the 3 observation monkeys, Ol. (*g*) Averaged map from the right hemispheres of the 3 observation monkeys, Or. Other conventions as in Figure 2.

of the IPs, its fundus and its posterior crown for the dorsoventral dimension. For the anteroposterior dimension, the distances used were those between the cytoarchitectonically identified borders of LIP dorsal and LIP ventral for the lateral bank, and those between the functionally identified border of PEip and the cytoarchitectonic borders of area MIP for the medial bank (Fig. 3*b*). Finally, the reference map of landmarks in the parietoccipital cortex was generated similarly (Fig. 4*a*,*b*). The distances used here were those between the surface landmarks of the medial parietoccipital sulcus (POm) and the medial and lateral crowns of POs as well as those between the cytoarchitectonic borders of V6 and V6A (Fig. 4*b*, white lines). Each individual cortical map with its own segments' landmarks was linearly transformed in Matlab (MathWorks, Inc., Natick, MA) to match the reference map. With this procedure, although the total surface of an area may change when it is geometrically normalized, the intensity and the spatial distribution of LCGU effects are preserved within it because these effects are proportionally shrunk or expanded within its borders. The geometrically normalized maps were used 1) to obtain average-LCGU maps out of control or experimental hemispheres and 2) to subtract control from experimental averaged maps.

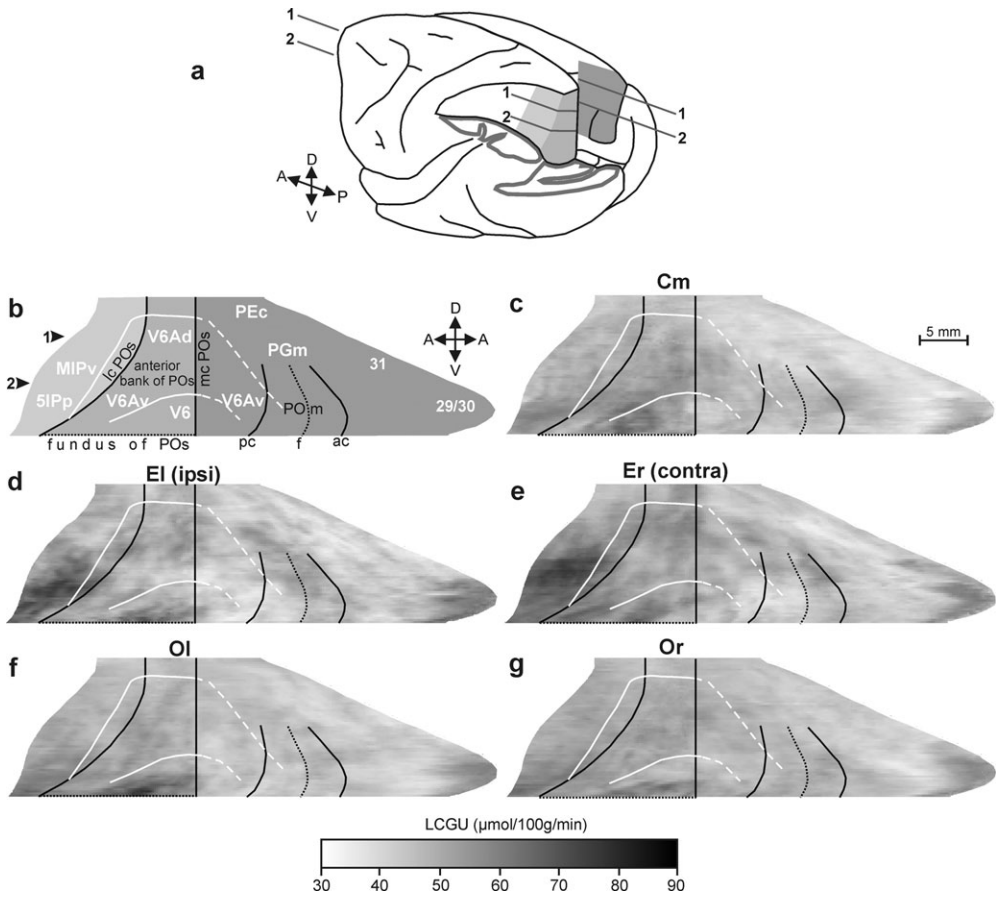

Figure 4. Quantitative 2D-maps of metabolic activity in the medial parietal and parietoccipital cortex. (*a*) Postero-lateral view of the partly dissected left hemisphere of a monkey brain with partial view of its mesial surface. The IPL was cut away at the level of the fundus of the IPs to show the cortex of the medial bank of this sulcus. The occipital lobe of the same hemisphere was also cut away at the level of the fundus of the POs and the Ls to show the cortex of the anterior bank of POs. Shaded area represents the reconstructed cortex including part of the medial bank of IPs, the anterior bank of POs and the adjacent part of the medial parietal cortex. (*b*) Schematic illustration of the geometrically normalized reconstructed cortical field. Different shades of gray correspond to those in panel a. Black lines represent surface landmarks, solid and interrupted white lines represent cytoarchitectonically and functionally identified borders, respectively, of the labeled cortical areas. The vertical black line in the middle of the reconstructed field depicts the medial crown of the anterior bank of POs (mc POs), point of alignment of the serial horizontal sections. The black line on its left demarcates the lateral crown of POs (lc POs) which partially corresponds to the intersection of the 3 sulci: IPs, POs and Ls. POm, medial parietoccipital sulcus, which is unfolded, with labeled its anterior crown (ac), fundus (f), and posterior crown (pc). (*c*) Averaged map from the 2 hemispheres of the motion-control monkey, Cm. (*d*) Averaged map from the left hemispheres of the 2 execution monkeys, El (ipsi). (*e*) Averaged map from the right hemispheres (contralateral to the moving forelimb) of the same monkeys, Er (contra). (*f*) Averaged map from the left hemispheres of the 3 observation monkeys, Ol. (*g*) Averaged map from the right hemispheres of the same monkeys, Or. POm, medial parietoccipital sulcus. Other conventions as in Figure 2.

Statistical Analysis

The average-LCGU values were calculated in sets of 5 adjacent sections (20 µm thick) throughout each cortical area of interest in each hemisphere. Experimental (E and O) to control (Cm) LCGU values were compared for statistical significances by the Student's unpaired *t*-test. Given that ipsilateral to contralateral LCGU values in normal control monkeys range up to 7% (Kennedy et al. 1978), only differences from the Cm higher than 7% were considered for statistical treatment (Bakola et al. 2006). The percent LCGU differences between the experimental (E and O) and the control (Cm) monkeys were generated using the formulae (E – Cm)/Cm × 100 and (O – Cm)/Cm × 100.

Results

All monkeys were trained for several months before the ^{14}C-DG experiment to perform their tasks continuously for at least 1 h/day. On the day of the ^{14}C-DG experiment, monkeys performed their tasks for the entire experimental period (45 min) without any breaks, and successful completion of each trial was rewarded with water. Success rate remained roughly constant (>90%) throughout the experiment. The mean rate of movements was similar for the execution and the observation tasks, as well as for the arm-motion control. To examine whether the differences in the performance of animals could influence our results, we compared the glucose consumption of the affected cortical areas between the 2 E monkeys which displayed a 33% difference in performance (executing 8 and 12 movements per min, respectively). This comparison showed that the differences in glucose consumption ranged between 4% and 9%, despite the fact that the performance differed by 33%. Apparently, the activation of the task-related areas in 2 different monkeys is similar provided that their task-performance exceeds a certain threshold. The amount of time that the monkeys spent fixating within the window of the behavioral apparatus during the critical 10 first minutes of the ^{14}C-DG experiment ranged between 6 and 7 min. For the rest of the time, the animals did not display any systematic oculomotor behavior that could account for false-positive effects in oculomotor related areas. In other words the line of sight of all the experimental monkeys was at random positions throughout the entire oculomotor space, same way as that of the biological motion control.

During the critical 10 first minutes of the ^{14}C-DG experiment, the Cm monkey observed 9 movements of the experimenter's arm per min and fixated within the window of the behavioral apparatus for 6 min. Because we found no significant interhemispheric difference of glucose consumption in any parietal area of the Cm monkey, the quantitative glucograms (maps of LCGU) of the cortex of the parietal convexity (Fig. 2*c*), the intraparietal cortex (Fig. 3*c*) and the parietoccipital/medial parietal cortices (Fig. 4*c*) of one side were averaged with the corresponding ones of the other side. The averaged glucogram of this monkey was used for measurement of control LCGU values in cortical areas of interest and comparisons with the experimental monkeys (Table 1).

The E monkeys executed an average of 10 movements per min during the critical 10 first minutes of the ^{14}C-DG experiment and fixated within the window of the behavioral apparatus for 7 min. We generated glucograms of the parietal convexity (Fig. 2*d*), the intraparietal (Fig. 3*d*) and the parietoccipital (Fig. 4*d*) cortices by averaging the 2 corresponding geometrically normalized glucograms in the left hemispheres (ipsilateral to the moving forelimb) of the 2 E monkeys. The latter glucograms as well as the equivalent ones in the right hemispheres (Figs 2*e*, 3*e*, and 4*e*, contralateral to the moving forelimb) were used for measurement of the LCGU values in cortical areas of interest, their statistical comparisons, and the estimation of the percent differences from the corresponding values of the Cm monkey (Table 1).

The O monkeys observed an average of 12 movements per min during the critical 10 first minutes of the ^{14}C-DG experiment and fixated within the window of the apparatus for 7 min. We generated glucograms of the parietal convexity (Fig. 2*f*), the intraparietal (Fig. 3*f*) and the parietoccipital (Fig. 4*f*) cortices by averaging the 3 corresponding, geometrically normalized glucograms in the left hemispheres of the 3 O monkeys. The latter glucograms as well as the equivalent ones in the right hemispheres (Figs 2*g*, 3*g*, and 4*g*) were used for measurement of the LCGU values in cortical areas of interest, their statistical comparisons, and the estimation of the percent differences from the Cm respective values (Table 1).

To illustrate the percent LCGU differences between the E monkeys and the Cm, we generated images of the spatio-intensive pattern of distribution of the metabolic activations, using the formula (E – Cm)/Cm × 100 for each one of the parietal-convexity, intraparietal and parietoccipital cortical glucograms. When the averaged maps of the parietal-convexity cortex in the left or in the right hemispheres of the E monkeys are compared with the corresponding averaged map of the Cm monkey (Fig. 5*a*,*b*, respectively), increased metabolic activity (net activation) is apparent in several cortical regions (see also Table 1). Superior parietal areas activated for execution of grasping movements include the widespread forelimb representation of SI-convexity (Pons et al. 1985) and area PEc contralaterally to the grasping forelimb, as well as area PE lateral (corresponding to the forelimb representation in area 5

Table 1
Metabolic effects in parietal cortical areas of the monkey brain

Cortical area	*n*	Cm (LCGU ± SD)	El (LCGU ± SD)	Er (LCGU ± SD)	Ol (LCGU ± SD)	Or (LCGU ± SD)	El/Cm (%)	Er/Cm (%)	Ol/Cm (%)	Or/Cm (%)
SPL										
SI convexity—pcd	32	52 ± 1	62 ± 3	61 ± 2	54 ± 1	55 ± 1	**19**	**17**	4	6
SI convexity—forelimb	48	56 ± 3	55 ± 5	65 ± 4	56 ± 4	61 ± 3	−2	**16**	0	**9**
SI convexity—forelimb (max)	20	53 ± 2	53 ± 2	65 ± 2	57 ± 2	63 ± 2	0	**23**	**8**	**19**
PE lateral (5-forelimb)	17	49 ± 1	53 ± 1	57 ± 1	53 ± 2	53 ± 1	**8**	**16**	**8**	**8**
PE medial	31	44 ± 1	48 ± 1	51 ± 2	47 ± 1	46 ± 1	**9**	**16**	7	5
PEc	28	43 ± 1	44 ± 2	50 ± 1	45 ± 1	47 ± 1	2	**16**	5	**9**
Medial intraparietal bank										
PEip anterior	102	49 ± 2	52 ± 2	60 ± 2	54 ± 2	57 ± 1	6	**22**	**10**	**16**
PEip middle	73	48 ± 1	48 ± 2	56 ± 2	50 ± 2	54 ± 1	0	**17**	4	**13**
PEip posterior dorsal (MIPd)	37	46 ± 1	48 ± 1	52 ± 2	47 ± 2	52 ± 1	4	**13**	2	**13**
PEip posterior ventral (MIPv)	35	48 ± 1	49 ± 3	57 ± 2	49 ± 1	52 ± 1	2	**19**	2	**8**
5IPp	53	53 ± 4	65 ± 4	67 ± 4	56 ± 4	56 ± 4	**23**	**26**	6	6
5VIP	28	47 ± 1	52 ± 1	54 ± 1	54 ± 1	54 ± 1	**11**	**15**	**15**	**15**
Lateral intraparietal bank										
AIP	45	49 ± 1	53 ± 1	60 ± 2	54 ± 3	51 ± 2	**8**	**22**	**10**	4
LIP dorsal	82	51 ± 2	55 ± 4	58 ± 5	52 ± 5	54 ± 3	**8**	**14**	2	6
LIP ventral	82	52 ± 2	50 ± 6	53 ± 7	51 ± 5	54 ± 5	−4	2	−2	4
LOP/CIP	102	51 ± 4	46 ± 7	47 ± 7	47 ± 4	51 ± 3	−10	−8	−8	0
7VIP	19	52 ± 1	59 ± 1	62 ± 1	61 ± 1	61 ± 1	**13**	**19**	**17**	**17**
Inferior parietal lobe										
PF	44	45 ± 2	45 ± 2	50 ± 2	50 ± 2	50 ± 1	0	**11**	**11**	**11**
PFG	57	44 ± 1	46 ± 2	51 ± 3	45 ± 1	45 ± 1	5	**16**	2	2
PG	59	43 ± 1	46 ± 3	50 ± 1	41 ± 3	45 ± 3	7	**16**	−5	5
Opt	44	43 ± 2	41 ± 2	44 ± 1	40 ± 2	44 ± 1	−5	2	−7	2
Anterior parieto-occipital bank										
V6Ad	34	48 ± 2	49 ± 1	54 ± 2	47 ± 1	49 ± 1	2	**13**	−2	2
V6Av	80	51 ± 1	47 ± 2	52 ± 2	49 ± 2	51 ± 1	−8	2	−4	0
V6 (max)	18	47 ± 2	51 ± 4	51 ± 2	55 ± 3	52 ± 3	**9**	**9**	**17**	**11**
Medial parietal areas										
PGm/7m (max)	66	42 ± 3	48 ± 3	50 ± 3	46 ± 2	46 ± 2	**14**	**19**	**10**	**10**
31 (max)	72	39 ± 1	40 ± 2	41 ± 1	42 ± 1	42 ± 1	3	5	**8**	**8**
Retrosplenial cortex (29/30)	69	41 ± 3	48 ± 8	48 ± 3	45 ± 4	46 ± 4	**17**	**17**	**10**	**12**

Note: *n*, number of sets of 5 adjacent horizontal sections used to obtain the mean LCGU values (in μmol/100 g/min) for each region. Cm values represent the average LCGU values from the 2 hemispheres of the motion-control monkey. El and Er values represent the average LCGU values from the 2 left and the 2 right hemispheres of the grasping-execution monkeys, respectively. Ol and Or values represent the average LCGU values from the 3 left and the 3 right hemispheres of the grasping-observation monkeys, respectively. SD, standard deviation of the mean. El/Cm, Er/Cm, Ol/Cm, Or/Cm, percent differences between El, Er, Ol, Or, and Cm, respectively, calculated as (experimental-control)/control × 100. pcd, postcentral dimple; (max), LCGU value in the region of maximal effect. Values in bold indicate statistically significant differences by the Student's unpaired *t*-test at the level of $P < 0.001$.

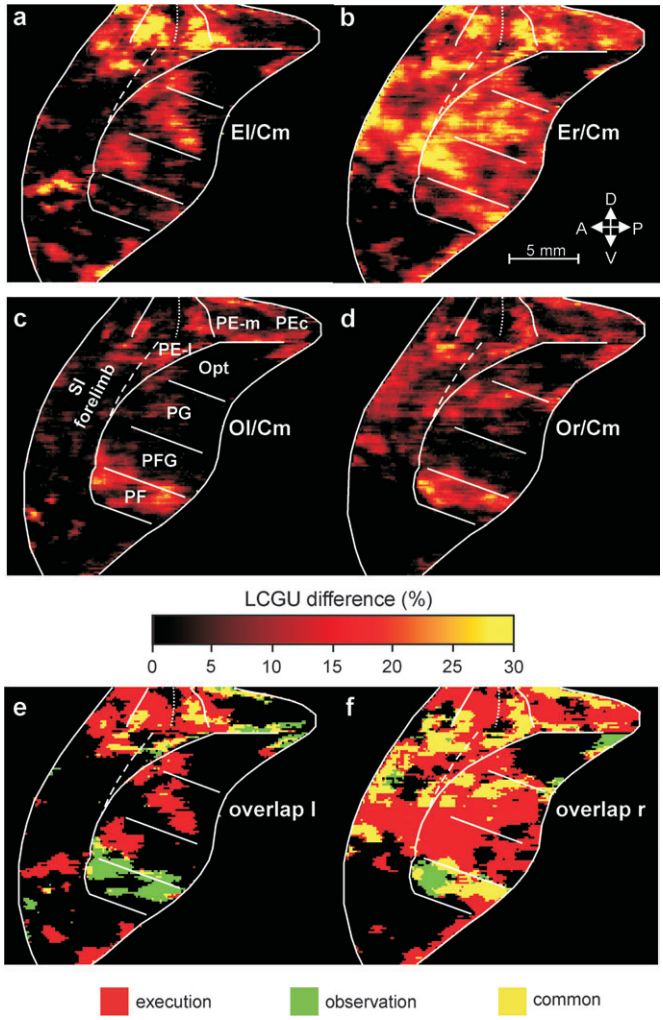

Figure 5. Lateral parietal cortical maps of percent LCGU differences from the motion control. Percent differences were calculated using the formula (E − Cm)/Cm × 100 for execution and (O − Cm)/Cm × 100 for observation. (*a*) Map of net execution-induced activations averaged from the left hemispheres of the 2 execution monkeys, El/Cm. (*b*) Map of net execution-induced activations averaged from the right hemispheres (contralateral to the moving forelimb) of the same monkeys, Er/Cm. (*c*) Map of net observation-induced activations averaged from the left hemispheres of the 3 observation monkeys, Ol/Cm. White lines correspond to the surface landmarks and the cytoarchitectonic borders of labeled areas, as in Figure 2. (*d*) Map of net observation-induced activations averaged from the right hemispheres of the observation monkeys, Or/Cm. Color bar indicates % LCGU differences from the Cm. (*e*) Superimposition of (*a*) and (*c*) panels. (*f*) Superimposition of (*b*) and (*d*) panels. In (*e*) and (*f*) panels, red and green represent activations higher than 10% induced by action execution and action observation, respectively. Yellow stands for activations induced by both execution and observation of the same action.

(Pons et al. 1985) and PE medial (corresponding to the trunk representation of area 5 (Pons et al. 1985) bilaterally (with more marked the contra- than the ipsilateral activations). Also bilaterally activated was found the trunk representation of area 2 around the pcd of only the E monkeys (Fig. 5, Table 1), presumably due to postural adjustments during reaching and grasping (Raos et al. 2004), whereas unaffected remained the mouth representation of the SI convexity at the ventralmost part of the reconstructions (Fig. 5). Inferior parietal areas activated for execution of reaching-to-grasp include the contralateral PF, PFG, and PG. When the averaged maps of the parietal-convexity cortex in the left and in the right hemispheres of the O monkeys are compared with the corresponding Cm map (Fig. 5*c*,*d*, respectively), observation-induced (net) activations are apparent in SI convexity-forelimb representation and area PEc of the right hemispheres, as well as in area PE lateral (or 5-forelimb) and PF bilaterally (see also Table 1). It should be noted that the latter 2 activations and the maximally activated region (max) within the SI convexity-forelimb representation displayed smaller interhemispheric differences in the O than in the E monkeys (Table 1).

When the averaged maps of the IPs cortex in the left or in the right hemispheres of the E monkeys are compared with the corresponding averaged map of the Cm monkey (Fig 6*a*,*b*, respectively), increased activity is apparent in several cortical regions (see also Table 1). Areas activated for execution of reaching-to-grasp in the medial intraparietal bank include the anterior and middle PEip and the dorsal and ventral MIP contralaterally to the grasping forelimb, as well as the 5VIP and the 5IPp bilaterally. Area 5IPp is an area we report for the first time, which does not correspond to any region previously described in the literature. It occupies the caudalmost and ventralmost region of the medial bank of the IPs. It is located rostral to area PIP, which has been described in the most anterior and lateral part of POs (Colby et al. 1988). Area 5IPp is ventrally demarcated by the fundus of IPs and borders areas MIP dorsally, 5VIP rostrally and V6A caudally. Interestingly, 5IPp displayed the highest parietal activation for grasping execution in the present study, but no effect during action observation. Of interest is also that the activations in the anterior and middle PEip of the medial bank of the IPs are distributed in anteroposterior (parallel to the crown) bands, which are very similar to those described in the past as projection bands from the SI-forelimb representation (Pearson and Powell 1985). In the lateral intraparietal bank, areas activated for execution of grasping include the AIP, the dorsal LIP and the 7VIP bilaterally, with the contralateral activations more marked than the ipsilateral ones. When the averaged maps of the IPs cortex in the left and in the right hemispheres of the O monkeys are compared with the corresponding Cm map (Fig. 6*c*,*d*, respectively), observation-induced activation is apparent in medial intraparietal areas such as the middle PEip and the dorsal and ventral MIP of the right hemispheres, as well as in the anterior PEip and the 5VIP bilaterally. Observation-induced activations also include the lateral intraparietal areas AIP of the left hemispheres and the 7VIP bilaterally. It should be noted that activations in areas 5VIP and 7VIP display no interhemispheric differences in the O monkeys (Table 1). A consistently significant depression was measured in an area corresponding to LOP or CIP in both hemispheres of the E monkeys and in the left hemispheres of the O monkeys (Table 1).

Finally, when the Cm map of the POs cortex is compared with the corresponding averaged maps in the left and the right hemispheres of the E monkeys (Fig. 7*a*,*b*, respectively), execution-induced activations are apparent in a portion of area V6 around the medial crown of the POs bilaterally, in the dorsal V6A contralaterally to the grasping hand, as well as in the PGm/7m and the retrosplenial cortical areas 29 and 30 bilaterally. When the Cm map of the POs cortex is compared with the corresponding averaged maps in the left and the right hemispheres of the O monkeys (Fig. 7*c*,*d*, respectively), observation-induced activations are apparent bilaterally in the same part of area V6 which was affected by execution, and in areas PGm/7m, 31, and 29/30 of the retrosplenial cortex (see also Table 1).

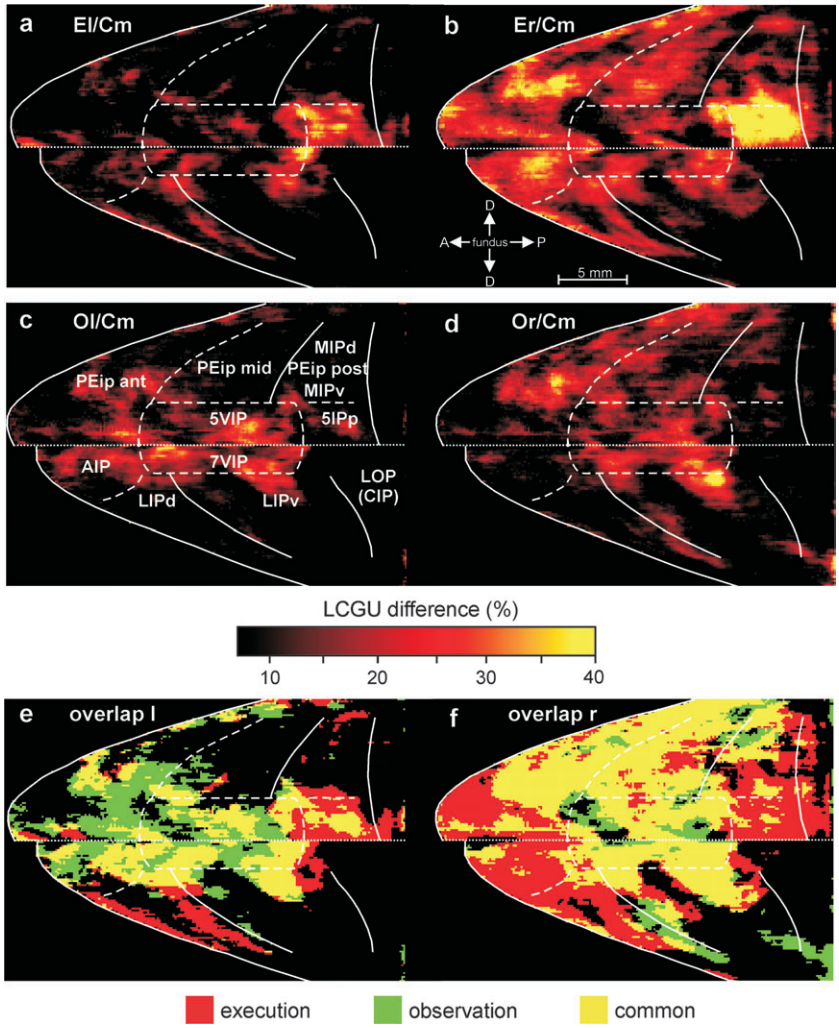

Figure 6. Intraparietal cortical maps of percent LCGU differences from the motion control. (*a*) Map of net execution-induced activations averaged from the left hemispheres of the 2 execution monkeys, El/Cm. (*b*) Map of corresponding activations averaged from the right hemispheres (contralateral to the moving forelimb) of the same monkeys, Er/Cm. (*c*) Map of net observation-induced activations averaged from the left hemispheres of the 3 observation monkeys, Ol/Cm. White lines correspond to the surface landmarks and the cytoarchitectonic borders of labeled areas, as in Figure 3. (*d*) Map of corresponding activations averaged from the right hemispheres of the 3 observation monkeys, Or/Cm. (*e*) Superimposition of panels (*a*) and (*c*). (*f*) Superimposition of panels (*b*) and (*d*). Other conventions as in Figure 5.

When spatially compared by superimposition, the observation-induced activations were found to overlap the execution-induced ones, partially in the parietal (Fig. 5*e*,*f*), largely in the intraparietal (Fig. 6*e*,*f*) and considerably in the parietoccipital cortex (Fig. 7*e*,*f*). In the above mentioned figures, red, green and yellow correspond to execution-induced, observation-elicited, and common activations, respectively. The distribution of activations for action execution differed from those for action observation in a more or less general pattern. To graphically illustrate the spatio-intensive (quantitative) distribution of metabolic activity within the affected regions, we plotted the differences between the experimental monkeys and the Cm (as % LCGU values and 95% confidence intervals per 100 μm) across the rostrocaudal extent in the reconstructed maps (Figs 8–10). The plots in these figures represent the percent differences between the E and the Cm monkeys (red lines) as well as between the O and the Cm monkeys (green lines). Baseline indicates 0% difference from the Cm. The plot in Figure 8 represents differences in the inferior parietal cortex along the ribbon highlighted in the schematic representation of the reconstructed cortex above the graph. In the left hemispheres of the 2 E monkeys ipsilateral to the grasping hand (dotted red line), activity is similar to that of the corresponding areas in the Cm (fluctuating around 0%). In contrast, significantly larger activations were found within areas PF, PFG, and PG (but not Opt) of the hemispheres contralateral to the grasping hand (Fig. 8, solid red line), resulting in a pronounced interhemispheric difference in the E monkeys. Interestingly, there is no interhemispheric difference in the activated PF of the O monkeys (Fig. 8, distance between the solid and the dotted green lines within PF). Consequently, the inferior parietal activations induced by action execution are contralateral to the grasping forelimb, in contrast to the PF activation elicited by action observation which is bilateral (see also Table 1).

The plots in Figure 9 represent differences from Cm in 4 subdivisions of the intraparietal cortex indicated by the ribbons of different gray-shades (Fig. 9*a*: ribbons b, c, d, and e), as highlighted in the schematic representation of the reconstructed cortex above the graphs. Graphs in panel b represent

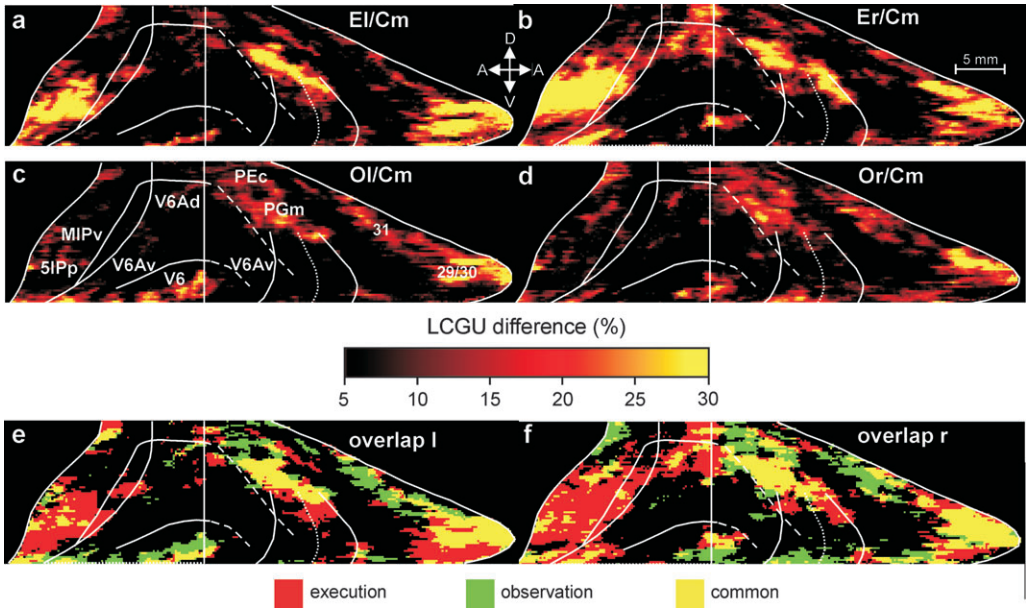

Figure 7. Medial parietal and parietoccipital cortical maps of percent LCGU differences from the motion control. (*a*) Map of net execution-induced activations averaged from the left hemispheres of the 2 execution monkeys, El/Cm. (*b*) Map of corresponding activations averaged from the right hemispheres (contralateral to the moving forelimb) of the same monkeys, Er/Cm. (*c*) Map of net observation-induced activations averaged from the left hemispheres of the 3 observation monkeys, Ol/Cm. White lines correspond to the surface landmarks and the cytoarchitectonic borders of labeled areas, as in Fig. 4. (*d*) Map of corresponding activations averaged from the right hemispheres of the 3 observation monkeys, Or/Cm. (*e*) Superimposition of panels (*a*) and (*c*). (*f*) Superimposition of panels (*b*) and (*d*). Other conventions as in Figure 5.

the 3 portions of area PEip (anterior, middle and posterior) in the medial bank of the IPs, as demarcated by the b-ribbon in panel (*a*). It is demonstrated that in the left hemispheres of the 2 E monkeys ipsilateral to the grasping hand (dotted red line) activity is similar to that of the corresponding areas in the Cm (fluctuating around zero), in contrast to the significant activations in the hemispheres contralateral to the grasping hand (solid red line), resulting in a pronounced interhemispheric difference in the E monkeys (distance between dotted and solid red lines). Interestingly, a much smaller interhemispheric difference is illustrated in the PEip of the O monkeys (Fig. 9*b*, distance between the solid and the dotted green lines smaller than that between the corresponding red lines). Moreover, in the O monkeys the PEip divisions are less activated than the corresponding areas of the affected hemisphere (contralateral to the grasping forelimb) of the E monkeys (Fig. 9*b*, Table 1). The plots in Figure 9*c* demonstrate the pattern of activations in areas 5VIP and 5IPp. The plots in Figure 9*d* demonstrate the 7VIP activation and the LOP/CIP inhibition. The plots in Figure 9*e* illustrate the activations in AIP and LIP. Finally, the plots in Figure 10 illustrate the activation of the contralateral V6A-dorsal in the E monkeys, the bilateral activations of the PGm/7m and the retrosplenial cortex in both the E and O cases, and the bilateral activation of area 31 in the O monkeys. In general, activations are higher in the E monkeys, and interhemispheric differences are smaller in the O monkeys (see also Table 1).

Discussion

The present quantitative neuroimaging study, combined with cytoarchitectonic identification of cortical areas, demonstrates the considerable overlap of the action execution and action observation networks in superior, inferior, and medial parietal cortical areas, which are thought to be involved in visuospatial attention, target selection for arm and eye movements, processing of visuomanual information, arm reaching, and object manipulation. At this point it should be noted that, although the activation of specific areas reflects their unequivocal involvement in action execution and/or in action observation in our study, the overlapping activations for execution and observation do not necessarily indicate involvement of the same cell populations in the 2 conditions.

Lateral Parietal Cortex

The lateralization of activation in the SI-forelimb representation of the SPL (corresponding to Brodmann's areas 1 and 2) contralateral to the moving forelimb of the E monkeys is compatible with classical knowledge and our previous reports (Savaki and Dalezios 1999; Raos et al. 2004; Gregoriou et al. 2005). The equivalent SI-forelimb activation in the SPL of the O monkeys mimics the results of previous reports demonstrating that the SI-forelimb activity within the Cs (corresponding mainly to areas 3a and 3b) was enhanced not only during manipulative hand actions but also during the observation of the same actions performed by another subject (Avikainen et al. 2002; Raos et al. 2004). The present results provide additional support to our earlier suggestion that overlapping somatosensory–motor neural correlates are responsible for motor program execution and motor percept creation (Raos et al. 2004, 2007). Moreover, the present results confirm that the activations induced by grasping execution and grasping observation in the SI-forelimb regions have similar patterns of distribution but different metabolic intensities. As we found for the SI-forelimb representation in the Cs (Raos et al. 2004), the activation of the SI-forelimb representation in the superior parietal convexity induced by observation of grasping is about 50% weaker in intensity than that induced by execution of

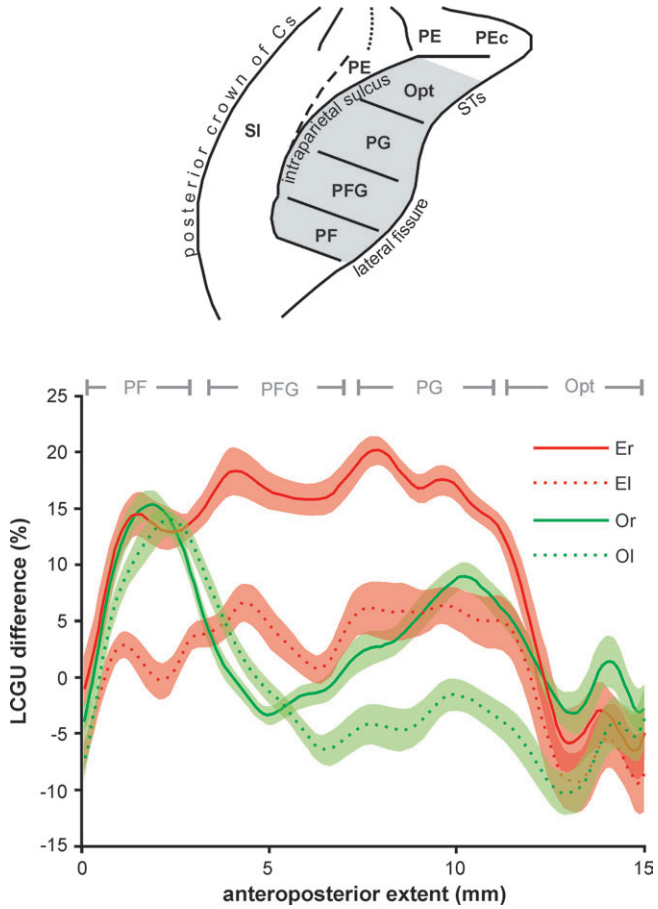

Figure 8. Plots of percent LCGU differences along the rostrocaudal extent of the reconstructed cortex of the inferior parietal convexity (along the ribbon highlighted in the drawing above the plots). The different areas corresponding to the various anteroposterior parts of the plots are labeled on top of the graphs. Red plots illustrate the differences between the 2 execution monkeys and the Cm. Green plots illustrate the differences between the 3 observation monkeys and the Cm. Plots with solid and dotted lines correspond to the right and the left hemispheres, respectively. Red and green shaded areas indicate 95% confidence intervals. Baseline corresponds to 0% LCGU difference from the Cm. Zero rostrocaudal extent represents the anterior border of PF. These plots illustrate the detailed spatio-intensive pattern of activation of PF, PFG and PG in the execution monkeys (activated only contralaterally to the moving forelimb), the bilateral activation of PF in the observation monkeys, and the smaller interhemispheric differences in the effects of the observation as compared with the execution monkeys. El, execution monkey left hemisphere; Er, execution right; Ol, observation left; Or, observation right.

grasping. As we have already suggested, the SI-forelimb activations during observation of actions may imply that subjects mentally rehearse the movements executed by others, and that the representation of movement is retrieved together with its somatosensory component. Indeed, in the absence of overt movement, EMG activation (Raos et al. 2004) and apparent sensory input, the SI-forelimb activation during observation of grasping may reflect the effects of mental simulation of this movement by the observer with prediction of the consequence of the movement (simultaneous recall of previous knowledge about the sensory effects). Finally, the fact that the SI-forelimb activation was found in the right superior parietal convexity of the O monkeys, that is, ipsilaterally to the experimenter's arm position and independently of the forelimb used in previous grasping experience of these monkeys (see Methods), is consistent with our previous results in the Cs (Raos et al. 2004) and with the right hemisphere dominance for visuospatial processes relative to movements (Chua et al. 1992; Decety 1996). Our findings that areas PE and PEc are involved in both execution and observation of grasping confirm previous reports demonstrating that the SPL contains a sensorimotor representation of the arm. On the sensory side, SPL receives somatosensory afferents from area 2 of the primary sensory cortex (Jones et al. 1978) and probably visual afferents from area MIP of the IPs (Caminiti et al. 1996), thus being able to integrate information about hand position and targets for reaching. On the motor side, SPL has connections with the primary motor cortex (Jones et al. 1978), the lateral premotor (Marconi et al. 2001) and the supplementary motor area (Pandya and Seltzer 1982) and is processing information about movement kinematics (Kalaska et al. 1990; Ashe and Georgopoulos 1994). Interestingly, all the above mentioned areas connected with the SPL were found to be activated for both execution and observation of grasping in our study (see also Raos et al. 2007). Finally, the bilateral involvement of the lateral PE (corresponding to the forelimb representation in area 5 of the SPL) in both experimental cases indicates that there is relatively smaller bias toward contralateral responses in PE than in SI and PEc, for example, that there are more bilateral visual and/or somatosensory receptive fields in the former than in the latter areas. Indeed, a substantial number of neurons with bilateral RFs on the hand digits have been found clustered adjacent to and/or within the medial bank of IPs (Iwamura et al. 1994) in contrast to the SI and PEc neurons which display mostly contralateral RFs (Nelson et al. 1980; Breveglieri et al. 2006).

In the IPL, the lack of involvement of Opt in reaching-to-grasp execution and the involvement of PF, PFG, and PG contralaterally to the grasping hand are findings compatible with previous reports demonstrating that area Opt receives mainly visual and eye-related input, whereas areas PG and PFG are connected with extrastriate visual, superior parietal somatosensory and premotor areas related to the control of arm movements, and area PF receives input from SI area 2 and projects to PG, PFG, and premotor arm-related areas (Pandya and Seltzer 1982; Petrides and Pandya 1984; Andersen et al. 1990; Rozzi et al. 2005; Gregoriou et al. 2006). The parallel activations measured in the superior and inferior parietal cortical areas during reaching-to-grasp execution in our study complement the recently reported strong similarity of firing patterns between hand manipulation neurons in SPL and IPL (Gardner et al. 2007) and support the suggestion that the former may supply arm movement–related information to the latter parietal areas. In fact, it was recently demonstrated that SPL neurons combining retinal, eye- and arm-movement information displayed discharges which were stronger and earlier than those displayed by IPL neurons processing the same information, and thus it was suggested that SPL can be the source of input signals to IPL (Battaglia-Mayer et al. 2007). Of the inferior parietal cortical areas we examined, only PF was involved in observation of grasping, and it was activated bilaterally. This finding confirms a previous report that PF neurons discharged not only during execution of hand actions but also during the observation of similar actions made by another individual, and therefore were defined as "PF-mirror neurons" in analogy with the F5-mirror neurons with corresponding properties (Gallese et al. 2002). Interestingly, PF neurons' discharge depends on the final goal of the action

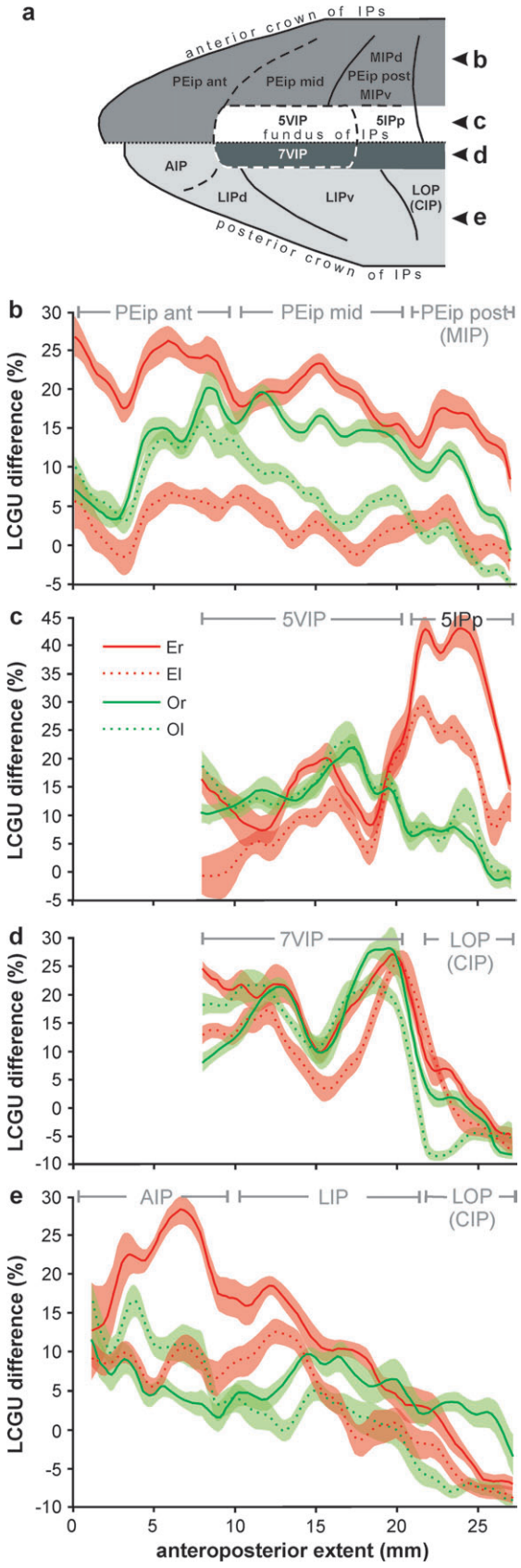

Figure 9. Plots of percent LCGU differences along the rostrocaudal extent of the reconstructed cortex in the IPs. Letters *b*–*e*, in the IPs drawing of the panel (*a*), label the different parts of cortex (differently shaded ribbons) which are plotted in the (*b*–*e*) panels, respectively. The different areas corresponding to the various anteroposterior parts of the plots are labeled on top of the graphs in each panel. Red plots illustrate the differences between the 2 execution monkeys and the Cm. Green plots illustrate the differences between the 3 observation monkeys and the Cm. Plots with solid and dotted lines correspond to the right and the left hemispheres, respectively. Red and green shaded areas indicate 95% confidence intervals. Baseline corresponds to 0% LCGU difference from the Cm. For example, the plots in panel b illustrate the detailed spatio-intensive pattern of activation of PEip contralaterally to the moving forelimb in the execution monkeys, the quantitatively less intense activation of PEip in the observation monkeys, and the smaller interhemispheric differences in the effects of the observation as compared with the execution monkeys. Other conventions as in Figure 8.

sequence in which grasping is embedded, thus probably encoding intention of movement (Fogassi et al. 2005). Additionally, in line with our finding that the PF is involved in action observation is the report that lesions of the IPL produced severe and selective impairments in motor imagery, that is, mental simulation of hand and finger movements (Sirigu et al. 1996).

All in all, our results confirm previous imaging studies of lower resolution which have demonstrated that superior and inferior parietal regions are involved in the observation of human actions (Bonda et al. 1996; Grafton et al. 1996; Decety et al. 1997; Grezes et al. 1998; Buccino et al. 2001). Moreover, they demonstrate the precise topography of these regions within the SPL and IPL of primates.

Intraparietal Cortex

The biggest part of the medial (or superior) bank of the IPs, corresponding to area 5, is occupied by area PEa (Pandya and Seltzer 1982) or PEip (Matelli et al. 1998). All the constituents of this area, that is, PEip anterior, PEip middle, and PEip posterior (the latter corresponding to area MIP) were activated in the E monkeys contralaterally to the grasping hand whereas areas 5IPp and 5VIP were bilaterally activated. The same medial intraparietal areas (with the single exception of 5IPp) were also activated in the O monkeys, demonstrating once again that there is an extensive overlap of the action execution and the action observation networks. Interestingly, areas PEip and VIP, herein documented to be involved in both action execution and action observation, are known to include proximal and distal forelimb representations with bimodal neurons characterized by visual receptive fields near the tactile ones (Jones et al. 1978; Colby and Duhamel 1991; Iriki et al. 1996; Duhamel et al. 1998) and to be connected with the premotor cortex (Matelli et al. 1998; Luppino et al. 1999; Lewis and Van Essen 2000a; Marconi et al. 2001) which is also involved in execution and observation of grasping (Raos et al. 2007). It should be noted that the 2 activated bands across the anterior and middle portions of area PEip in our reconstructions resemble the distribution of SI-forelimb projections to the medial bank of IPs (Jones et al. 1978) as well as the distribution of the 2 neuronal populations in the PEip sending afferents to the dorsal premotor F2-arm field (Matelli et al. 1998). These bands also resemble the zones activated for arm reaching to visual targets and for memory-guided reaching in the dark, zones which were associated with somatosensory guidance of movement and/or efference copy of motor command (Gregoriou and Savaki 2001). Also, the herein documented involvement of area MIP in execution and observation of reaching-to-grasp is compatible with reports that this area responds to visual and somatosensory stimuli, especially when visual stimuli are within reaching distance of the monkey (Colby and Duhamel

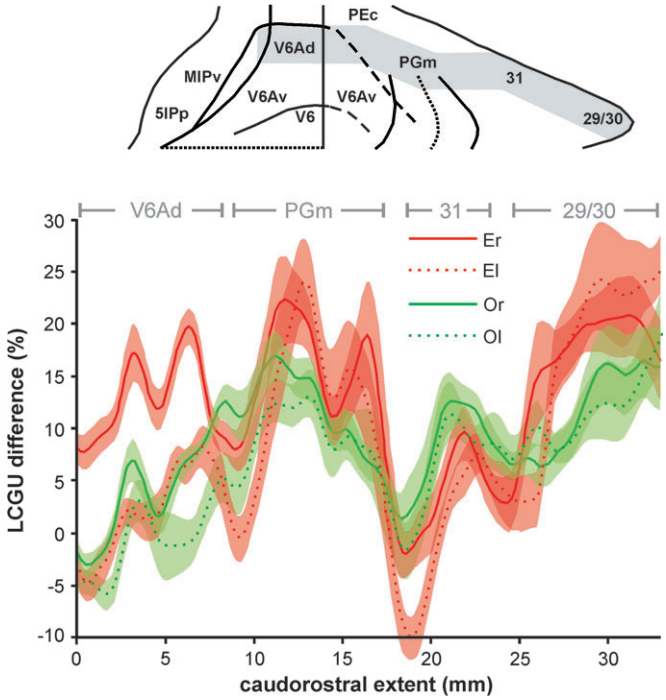

Figure 10. Plots of percent LCGU differences along the reconstructed cortex of the dorsal part of the anterior bank of POs and its adjacent medial parietal cortical field (along the ribbon highlighted in the drawing above the plots) including the dorsal part of V6A, areas PGm/7m, 31 and the retrosplenial cortical areas 29/30. Red plots illustrate the differences between the 2 execution monkeys and the Cm. Green plots illustrate the differences between the 3 observation monkeys and the Cm. Plots with solid and dotted lines correspond to the right and the left hemispheres, respectively. Red and green shaded areas indicate 95% confidence intervals. Baseline corresponds to 0% LCGU difference from the Cm. Zero rostrocaudal extent represents the anterior border of V6Ad. Other conventions as in Figure 8.

1991; Johnson et al. 1996), and receives a motor efference copy generated in relation to the preparation and/or execution of movement (for reviews see Andersen et al. 1997; Colby and Goldberg 1999). In general, the smaller activations that we found in the superior parietal convexity and the bigger and more bilateral activations in the medial bank of the IPs for action observation as compared with action execution are compatible with previous reports demonstrating that more dorsal SPL areas (around the convexity) are associated with movement- and position-related somatosensory activity whereas more ventral parts of the SPL (in the medial bank of the IPs) show more prominent visual activity (Colby and Duhamel 1991; Savaki et al. 1993; Johnson et al. 1996; Kalaska 1996; Graziano et al. 2000; Gregoriou and Savaki 2001). Area 5IPp in the caudalmost part of the medial bank of the IPs adjacent to the fundus, which displayed the strongest activation in the E monkeys and remained unaffected in the O monkeys, has not been previously reported. As explained in the Results section, this area may only partially correspond to the originally described area PIP (Colby et al. 1988) which is considered to be a motion sensitive area (Vanduffel et al. 2001; Durand et al. 2007) integrating shape information by cross-modal (tactile-visual) matching (Saito et al. 2003). Indeed, this cross-modal matching could take place only in the E monkeys.

In the lateral (or inferior) bank of the IPS, areas AIP and 7VIP are involved in both execution and observation of action whereas LIP dorsal is involved only in action execution. The bilateral involvement of area 7VIP in execution and observation of reaching-to-grasp supports our earlier suggestion that this region encodes visual information about the location of stimuli used as targets for motor acts, whatever the effector used (Gregoriou and Savaki 2001). The involvement of area AIP in both execution and observation of reaching-to-grasp is compatible with existing knowledge that its neurons are preferentially activated for various hand configurations during grasping of differently shaped objects (Sakata et al. 1995; Murata et al. 2000), and its pharmacological inactivation disrupts hand preshaping during grasping (Gallese et al. 1994). The AIP is a target of projections from area LOP/CIP (Nakamura et al. 2001) which was inhibited in our study, but it is also connected with area V6Ad (Borra et al. 2008) which was activated for execution, and with areas MIP and F5 (Petrides and Pandya 1984; Matelli et al. 1986; Luppino et al. 1999; Borra et al. 2008) which were activated for both execution and observation. Finally, our results confirm previous findings with imaging methods of lower resolutions, demonstrating that aIPS, the human equivalent of monkey AIP, is recruited on execution of grasping movements (Binkofski et al. 1998; Culham et al. 2003; Shmuelof and Zohary 2006), on an array of grasp observation tasks (Grafton et al. 1996; Hamilton et al. 2006; Shmuelof and Zohary 2006) and even on the perception of scripts of goal-directed hand actions (Bonda et al. 1996). As for area LIP, it is known that its neurons carry saccade-related signals (Gnadt and Andersen 1988; Duhamel et al. 1992) and their discharge is modulated by selective spatial attention (Duhamel et al. 1992; Gottlieb et al. 1998). Our finding that LIP dorsal but not LIP ventral is involved in visually guided reaching-to-grasp movements, is compatible with our recent report that the visual space is represented in LIP dorsal in contrast to the oculomotor space which is mainly represented in LIP ventral (Bakola et al. 2006). Furthermore, the bilateral involvement of 7VIP and 5VIP in action execution and observation complements a previous study demonstrating that there is an arm-reach-associated region which is located in 7VIP and extends to 5VIP (Gregoriou and Savaki 2001).

Our results confirm a recent imaging study of lower resolution, demonstrating that there is considerable overlap between areas activated for execution and observation of reaching movements in the SPL and the intraparietal sulcus in humans, and also that reaching activates these areas more than observation of reaching (Filimon et al. 2007). All existing data considered, the IPs cortex acts as a multifaceted behavioral integrator that binds information related not only to attention, visual and somatosensory space, oculomotor and skeletomotor activity but also to action recognition, thus operating at the interface of perception, action, and cognition.

Medial Parietal and Parietoccipital Cortex

The herein documented involvement of the visual area V6 in execution and observation of visually guided reaching-to-grasp movements is compatible with the knowledge that this area receives form- and motion-related visual inputs from the striate cortex and several extrastriate areas, and sends projections to arm-related areas such as MIP and V6A, as well as to areas encoding the spatial location of objects to be grasped such as VIP and V6A (Colby and Duhamel 1991; Duhamel et al. 1997; Galletti et al. 2001; Galletti et al. 2003). According to the retinotopic organization of its visual input, the peripheral field of V6 is represented medially and the central one laterally

(Galletti, Fattori, Gamberini, et al. 1999). Our finding that portions of both these fields of V6 are involved in reaching-to-grasp indicates that the monkeys were attending their arm approaching from the visual periphery to the center while fixating the object straight ahead. Interestingly, direction-selective (Galletti et al. 1996) and "real-motion" (Galletti and Fattori 2003) cells have been demonstrated in area V6. The dorsal part of the bimodal (visual/somatosensory) area V6A, herein found to be implicated in reaching-to-grasp execution, is known to contain more arm-related cells than its ventral counterpart (Fattori et al. 1999) which is not affected in our study. In fact, cells in V6A-dorsal modulate their activity during reaching to (Fattori et al. 2001, 2005) and grasping of (Fattori et al. 2004) objects in the peripersonal space. These cells are known to project to the dorsal premotor areas F2 and F7 (Matelli et al. 1998; Shipp et al. 1998; Marconi et al. 2001) and are thought to interact continuously with the premotor cortex in order to guide "on-line" the ongoing arm movement (Galletti et al. 2003).

In contrast to area V6A-dorsal involved only in execution, area PGm/7m which is the alternative visuomotor relay station receiving visual input and projecting to the dorsal premotor cortex (Petrides and Pandya 1984; Cavada and Goldman-Rakic 1989b; Johnson et al. 1996; Matelli et al. 1998) was involved not only in the execution but also in the observation of reaching-to-grasp. Our results are in agreement with previous reports demonstrating that cell activity in PGm/7m relates to a combination of visuomanual and oculomotor information supposedly leading from target localization to movement generation (Ferraina, Johnson, et al. 1997), with the composition of motor commands based on kinesthetic and visual control signals (Ferraina, Garasto, et al. 1997). Also, our results support a previous imaging study demonstrating that execution and observation of action involve an area between the POs and the posterior end of the cingulate sulcus (Binkofski et al. 1999), which apparently corresponds to PGm/7m. Of interest is that area F7, which receives the main parietal input from PGm/7m, as well as other major projecting areas of PGm/7m such as the supplementary somatosensory area, the cingulate cortex, area VIP and the retrosplenial cortex (Petrides and Pandya 1984; Cavada and Goldman-Rakic 1989b; Johnson et al. 1996; Matelli et al. 1998) are involved not only in execution but also in observation of reaching-to-grasp movements (see also Raos et al. 2007).

The bilateral involvement of the retrosplenial cortical areas 29 and 30 in both execution and observation of reaching-to-grasp is compatible with the suggestions that this region processes aspects of working memory (Petrides et al. 1993; Petrides 1995; Morris et al. 1999; Kobayashi and Amaral 2003) and is involved in the perception of visual objects associated with a specific context (Bar and Aminoff 2003). The bilateral involvement of area 31 in observation, is compatible with reports associating it with occulomotor activity in the service of the spatial analysis of visual input (Olson et al. 1996) and the motivational salience of visual and occulomotor events for orienting attention (Dean et al. 2004).

Mental Simulation of Action and Action Attribution

The overall finding that observing an action excites very similar parietal circuits used to execute that same action supports our earlier suggestion that observation of an action corresponds to simulation of its overt counterpart (Raos et al. 2007). Accordingly, to understand the action of another person the observer executes it "mentally." More specifically, the herein documented fact that the neural correlates of the action observation-driven system in the parietal cortex extend well beyond area PF where mirror neurons were found (Gallese et al. 2002), same way as those in the frontal cortex extend well beyond the F5-convexity (Raos et al. 2007) where the mirror neurons were originally discovered (Gallese et al. 1996; Rizzolatti et al. 1996), challenges the "mirror-neuron system" concept and supports the suggestion that a broader process such as "mental simulation of action" is responsible for action recognition (Goldman and Sebanz 2005). Hence, the present and our previous results (Raos et al. 2007) support the "mental simulation theory" which assigns the role of understanding others' actions to the entire distributed neural network responsible for the execution of actions, and not the concept of "mirroring" which reflects the function of a certain class of cells in premotor area F5 and parietal area PF.

A reasonable question is how we distinguish between the observer and the actor if we simulate the action when we observe it by recruiting the same circuits which are responsible for execution of the act. In a previous study, we argued that the attribution of an action to an agent is a function distributed within the action execution network rather than a function assigned to one or 2 areas on the side of this pathway. We also discussed, based on our results, how the primary motor and somatosensory, the premotor and supplementary somatosensory areas may contribute to the attribution of action to the other agent during action observation and to the self during action execution (Raos et al. 2007). In the parietal cortex, areas PG/PFG, LIPd, 5IPp, and V6Ad which are involved only in action execution and not in action observation, as well as area 31 which is involved in observation but and not in execution, may contribute in attributing the action to the self and to the other agent, respectively. Moreover, the parietal activations induced by action observation were in general weaker than those induced by action execution, suggesting a possible subthreshold activation of the action execution circuits during action observation. Also, the effects induced by action observation displayed smaller interhemispheric differences (indicative of visual rather than hand identity specificity) as compared with those induced by action execution which were mostly contralateral to the moving forelimb (preserving hand identity specificity). These differential activations of parietal cortical areas could also play a role in attributing the action to the correct agent.

For example, in the forelimb-related areas of the parietal cortex, the higher level of activity for action execution may reflect the anticipated sensory consequence of the movement (based on efference copy of the motor command) and the actual afferent feedback (signal from the muscles), whereas the lower activity for action observation may reflect the anticipated consequence of the movement only. This interpretation of our results is compatible with previous suggestions such as that prediction (or anticipation) may turn motor commands into expected sensory consequences (Kilner et al. 2004, 2007), that prediction of the sensory consequences of an act may underlie our ability to distinguish between self-produced and externally generated actions (Blakemore and Frith 2003), and that the experience of ourselves or others as the cause of an action may be based on comparison of motor commands with the afferent feedback from the moving muscles and the external events

caused by these commands (Johnson and Haggard 2005), with the temporal attraction between self-produced actions and their sensory consequences binding them together and thus enhancing the experience of agency (Haggard et al. 2002).

There are several reports attributing to the parietal cortex a role in detecting conflicts between visual and somatomotor signals of motor acts (Fink et al. 1999; Farrer et al. 2003; Costantini et al. 2005), a role in action attribution (awareness of one's own movements versus movements of another agents) (Sirigu et al. 1999; Blakemore et al. 2003; Sirigu et al. 2004), and even more specifically assigning to the inferior parietal lobe and the intraparietal sulcus a role in the attribution of actions to external agents (Ruby and Decety 2001; Decety et al. 2002; Farrer and Frith 2002). However, our findings suggest that the parietal cortical areas associated with attribution of action in the above mentioned studies constitute central components of the execution/perception distributed network rather than extra machinery functioning on the side of this net.

In conclusion and all our results considered, observation of an action performed by another subject reflects the effects of our previous knowledge about the act and its predicted sensory consequences. During action observation, internally simulated experience of the specific movements recruits numerous parietofrontal sensory–motor cortical regions, mostly the same ones which are responsible for the execution of the same action. In addition, the parietal execution/perception system participates in the process of attribution of the action to the correct agent by integrating visual and effector-related somatosensory–motor inputs and thus by creating a coherent representation of the bodily self.

Funding

Greek Secretariat of Research and Technology (PENED grant 01ED111) supported Mina Evangeliou; and European Union (FP6 grant IST-027574).

Notes

We thank Helen Barbas, Michela Gamberini, Georgia Gregoriou, and Maya Medalla for advice and help regarding histology and Maria Kefaloyianni for help with the autoradiographic imaging. *Conflict of Interest*: None declared.

Address correspondence to Professor Helen E. Savaki, Department of Basic Sciences, Faculty of Medicine, School of Health Sciences, University of Crete, P.O. Box 2208, GR-71003, Iraklion, Crete, Greece. Email: savaki@med.uoc.gr.

References

Andersen RA. 1989. Visual and eye movement functions of the posterior parietal cortex. Annu Rev Neurosci. 12:377–403.

Andersen RA, Asanuma C, Essick G, Siegel RM. 1990. Corticocortical connections of anatomically and physiologically defined subdivisions within the inferior parietal lobule. J Comp Neurol. 296:65–113.

Andersen RA, Snyder LH, Bradley DC, Xing J. 1997. Multimodal representation of space in the posterior parietal cortex and its use in planning movements. Annu Rev Neurosci. 20:303–330.

Ashe J, Georgopoulos AP. 1994. Movement parameters and neural activity in motor cortex and area 5. Cereb Cortex. 4:590–600.

Avikainen S, Forss N, Hari R. 2002. Modulated activation of the human SI and SII cortices during observation of hand actions. Neuroimage. 15:640–646.

Bakola S, Gregoriou GG, Moschovakis AK, Savaki HE. 2006. Functional imaging of the intraparietal cortex during saccades to visual and memorized targets. Neuroimage. 31:1637–1649.

Bar M, Aminoff E. 2003. Cortical analysis of visual context. Neuron. 38:347–358.

Battaglia-Mayer A, Mascaro M, Caminiti R. 2007. Temporal evolution and strength of neural activity in parietal cortex during eye and hand movements. Cereb Cortex. 17:1350–1363.

Binkofski F, Buccino G, Posse S, Seitz RJ, Rizzolatti G, Freund H. 1999. A fronto-parietal circuit for object manipulation in man: evidence from an fMRI-study. Eur J Neurosci. 11:3276–3286.

Binkofski F, Dohle C, Posse S, Stephan KM, Hefter H, Seitz RJ, Freund HJ. 1998. Human anterior intraparietal area subserves prehension: a combined lesion and functional MRI activation study. Neurology. 50:1253–1259.

Blakemore SJ, Frith C. 2003. Self-awareness and action. Curr Opin Neurobiol. 13:219–224.

Blakemore SJ, Oakley DA, Frith CD. 2003. Delusions of alien control in the normal brain. Neuropsychologia. 41:1058–1067.

Bonda E, Petrides M, Ostry D, Evans A. 1996. Specific involvement of human parietal systems and the amygdala in the perception of biological motion. J Neurosci. 16:3737–3744.

Borra E, Belmalih A, Calzavara R, Gerbella M, Murata A, Rozzi S, Luppino G. 2008. Cortical connections of the macaque anterior intraparietal (AIP) area. Cereb Cortex. 18:1094–1111.

Breveglieri R, Galletti C, Gamberini M, Passarelli L, Fattori P. 2006. Somatosensory cells in area PEc of macaque posterior parietal cortex. J Neurosci. 26:3679–3684.

Buccino G, Binkofski F, Fink GR, Fadiga L, Fogassi L, Gallese V, Seitz RJ, Zilles K, Rizzolatti G, Freund HJ. 2001. Action observation activates premotor and parietal areas in a somatotopic manner: an fMRI study. Eur J Neurosci. 13:400–404.

Caminiti R, Ferraina S, Johnson PB. 1996. The sources of visual information to the primate frontal lobe: a novel role for the superior parietal lobule. Cereb Cortex. 6:319–328.

Cavada C, Goldman-Rakic PS. 1989a. Posterior parietal cortex in rhesus monkey: I. Parcellation of areas based on distinctive limbic and sensory corticocortical connections. J Comp Neurol. 287:393–421.

Cavada C, Goldman-Rakic PS. 1989b. Posterior parietal cortex in rhesus monkey: II. Evidence for segregated corticocortical networks linking sensory and limbic areas with the frontal lobe. J Comp Neurol. 287:422–445.

Chua R, Carson RG, Goodman D, Elliot D. 1992. Asymmetries in the spatial localization of transformed targets. Brain Cogn. 20:227–235.

Colby CL, Duhamel JR. 1991. Heterogeneity of extrastriate visual areas and multiple parietal areas in the macaque monkey. Neuropsychologia. 23:517–537.

Colby CL, Duhamel J-R, Goldberg ME. 1993. Ventral intraparietal area of the macaque: anatomic location and visual response properties. J Neurophysiol. 69:902–914.

Colby CL, Gattass R, Olson CR, Gross CG. 1988. Topographical organization of cortical afferents to extrastriate visual area PO in the macaque: a dual tracer study. J Comp Neurol. 269:392–413.

Colby CL, Goldberg ME. 1999. Space and attention in parietal cortex. Annu Rev Neurosci. 22:319–349.

Costantini M, Galati G, Ferretti A, Caulo M, Tartaro A, Romani GL, Aglioti SM. 2005. Neural systems underlying observation of humanly impossible movements: an fMRI study. Cereb Cortex. 15:1761–1767.

Culham JC, Danckert SL, DeSouza JF, Gati JS, Menon RS, Goodale MA. 2003. Visually guided grasping produces fMRI activation in dorsal but not ventral stream brain areas. Exp Brain Res. 153:180–189.

Dalezios Y, Raos VC, Savaki HE. 1996. Metabolic activity pattern in the motor and somatosensory cortex of monkeys performing a visually guided reaching task with one forelimb. Neuroscience. 72:325–333.

Dean HL, Crowley JC, Platt ML. 2004. Visual and saccade-related activity in macaque posterior cingulate cortex. J Neurophysiol. 92:3056–3068.

Decety J. 1996. Do imagined and executed actions share the same neural substrate? Brain Res Cogn Brain Res. 3:87–93.

Decety J, Chaminade T, Grezes J, Meltzoff AN. 2002. A PET exploration of the neural mechanisms involved in reciprocal imitation. Neuroimage. 15:265–272.

Decety J, Grezes J, Costes N, Perani D, Jeannerod M, Procyk E, Grassi F, Fazio F. 1997. Brain activity during observation of actions. Influence of action content and subject's strategy. Brain. 120:1763–1777.

Duhamel J-R, Bremmer F, SB, Graf W. 1997. Spatial invariance of visual receptive fields in parietal cortex neurons. Nature. 389:845–847.

Duhamel J-R, Colby CL, Goldberg ME. 1992. The updating of the representation of visual space in parietal cortex by intended eye movements. Science. 255:90–92.
Duhamel J-R, Colby CL, Goldberg ME. 1998. Ventral intraparietal area of the macaque: congruent visual and somatic response properties. J Neurophysiol. 79:126–136.
Durand JB, Nelissen K, Joly O, Wardak C, Todd JT, Norman JF, Janssen P, Vanduffel W, Orban GA. 2007. Anterior regions of monkey parietal cortex process visual 3D shape. Neuron. 55:493–505.
Farrer C, Franck N, Georgieff N, Frith CD, Decety J, Jeannerod M. 2003. Modulating the experience of agency: a positron emission tomography study. Neuroimage. 18:324–333.
Farrer C, Frith CD. 2002. Experiencing oneself vs another person as being the cause of an action: the neural correlates of the experience of agency. Neuroimage. 15:596–603.
Fattori P, Breveglieri R, Amoroso K, Galletti C. 2004. Evidence for both reaching and grasping activity in the medial parieto-occipital cortex of the macaque. Eur J Neurosci. 20:2457–2466.
Fattori P, Gamberini M, Kutz DF, Galletti C. 2001. 'Arm-reaching' neurons in the parietal area V6A of the macaque monkey. Eur J Neurosci. 13:2309–2313.
Fattori P, Gamberini M, Mussio A, Breveglieri R, Kutz DF, Galletti C. 1999. A visual-to-motor gradient within area V6A of the monkey parieto-occipital cortex. Neurosci Lett Suppl. 52:S22.
Fattori P, Kutz DF, Breveglieri R, Marzocchi N, Galletti C. 2005. Spatial tuning of reaching activity in the medial parieto-occipital cortex (area V6A) of macaque monkey. Eur J Neurosci. 22:956–972.
Ferraina S, Garasto MR, Battaglia-Mayer A, Ferraresi P, Johnson PB, Lacquaniti F, Caminiti R. 1997. Visual control of hand-reaching movement: activity in parietal area 7m. Eur J Neurosci. 9:1091–1095.
Ferraina S, Johnson PB, Garasto MR, Battaglia-Mayer A, Ercolani L, Bianchi L, Lacquaniti F, Caminiti R. 1997. Combination of hand and gaze signals during reaching: activity in parietal area 7m of the monkey. J Neurophysiol. 77:1034–1038.
Filimon F, Nelson JD, Hagler DJ, Sereno MI. 2007. Human cortical representations for reaching: mirror neurons for execution, observation, and imagery. Neuroimage. 37:1315–1328.
Fink GR, Marshall JC, Halligan PW, Frith CD, Driver J, Frackowiak RSJ, Dolan RJ. 1999. The neural consequences of conflict between intention and the senses. Brain. 122:497–512.
Fogassi L, Ferrari PF, Gesierich B, Rozzi S, Chersi F, Rizzolatti G. 2005. Parietal lobe: from action organization to intention understanding. Science. 308:662–667.
Gallese V, Fadiga L, Fogassi L, Rizzolatti G. 1996. Action recognition in the premotor cortex. Brain. 119:593–609.
Gallese V, Fadiga L, Fogassi L, Rizzolatti G. 2002. Action representation and the inferior parietal lobe. In: Prinz W, Hommel B, editors. Common mechanisms in perception and action: attention and performance. Oxford: Oxford University Press. p. 334–355.
Gallese V, Murata A, Kaseda M, Niki N, Sakata H. 1994. Deficit of hand preshaping after muscimol injection in monkey parietal cortex. Neuroreport. 5:1525–1529.
Galletti C, Fattori P. 2003. Neuronal mechanisms for detection of motion in the field of view. Neuropsychologia. 41:1717–1727.
Galletti C, Fattori P, Battaglini PP, Shipp S, Zeki S. 1996. Functional demarcation of a border between areas V6 and V6A in the superior parietal gyrus of the macaque monkey. Eur J Neurosci. 8:30–52.
Galletti C, Fattori P, Gamberini M, Kutz DF. 1999. The cortical visual area V6: brain location and visual topography. Eur J Neurosci. 11:3922–3936.
Galletti C, Fattori P, Kutz DF, Gamberini M. 1999. Brain location and visual topography of cortical area V6A in the macaque monkey. Eur J Neurosci. 11:575–582.
Galletti C, Gamberini M, Kutz DF, Fattori P, Luppino G, Matelli M. 2001. The cortical connections of area V6: occipito- parietal network processing visual information. Eur J Neurosci. 13:1–18.
Galletti C, Kutz DF, Gamberini M, Breveglieri R, Fattori P. 2003. Role of the medial parieto-occipital cortex in the control of reaching and grasping movements. Exp Brain Res. 153:158–170.
Gardner EP, Babu KS, Reitzen SD, Ghosh S, Brown AS, Chen J, Hall AL, Herzlinger MD, Kohlenstein JB, Ro JY. 2007. Neurophysiology of prehension. I. Posterior parietal cortex and object-oriented hand behaviors. J Neurophysiol. 97:387–406.
Gnadt JW, Andersen RA. 1988. Memory related motor planning activity in posterior parietal cortex of macaque. Exp Brain Res. 70:216–220.
Goldman AI, Sebanz N. 2005. Simulation, mirroring, and a different argument from error. Trends Cogn Sci. 9:320.
Gottlieb JP, Kusunoki M, Goldberg ME. 1998. The representation of visual salience in monkey parietal cortex. Nature. 391:481–484.
Grafton ST, Arbib MA, Fadiga L, Rizzolatti G. 1996. Localization of grasp representations in humans by positron emission tomography. 2. Observation compared with imagination. Exp Brain Res. 112:103–111.
Graziano MSA, Cooke DF, Taylor CSR. 2000. Coding the location of the arm by sight. Science. 290:1782–1786.
Gregoriou GG, Borra E, Matelli M, Luppino G. 2006. Architectonic organization of the inferior parietal convexity of the macaque monkey. J Comp Neurol. 496:422–451.
Gregoriou GG, Luppino G, Matelli M, Savaki HE. 2005. Frontal cortical areas of the monkey brain engaged in reaching behavior: a (14)C-deoxyglucose imaging study. Neuroimage. 27:442–464.
Gregoriou GG, Savaki HE. 2001. The intraparietal cortex: subregions involved in fixation, saccades, and in the visual and somatosensory guidance of reaching. J Cereb Blood Flow Metab. 21:671–682.
Gregoriou GG, Savaki HE. 2003. When vision guides movement: a functional imaging study of the monkey brain. Neuroimage. 19:959–967.
Grezes J, Costes N, Decety J. 1998. Top-down effect of strategy on the perception of human biological motion: a PET investigation. Cogn Neuropsychol. 15:553–582.
Haggard P, Clark S, Kalogeras J. 2002. Voluntary action and conscious awareness. Nat Neurosci. 5:382–385.
Hamilton AF, Wolpert DM, Frith U, Grafton ST. 2006. Where does your own action influence your perception of another person's action in the brain? Neuroimage. 29:524–535.
Iriki A, Tanaka M, Iwamura Y. 1996. Coding of modified body schema during tool use by macaque postcentral neurons. Neuroreport. 7:2325–2330.
Iwamura Y, Iriki A, Tanaka M. 1994. Bilateral hand representation in the postcentral somatosensory cortex. Nature. 369:546–554.
Johnson H, Haggard P. 2005. Motor awareness without perceptual awareness. Neuropsychologia. 43:227–237.
Johnson PB, Ferraina S, Bianchi L, Caminiti R. 1996. Cortical networks for visual reaching: Physiological and anatomical organization of frontal and parietal lobe arm regions. Cereb Cortex. 6:102–119.
Jones EG, Coulter JD, Hendry HC. 1978. Intracortical connectivity of architectonic fields in the somatic sensory, motor and parietal cortex of monkeys. J Comp Neurol. 181:291–348.
Kalaska JF. 1996. Parietal cortex area 5 and visuomotor behavior. Can J Physiol Pharmacol. 74:483–498.
Kalaska JF, Cohen DAD, Prud'homme M, Hyde ML. 1990. Parietal area 5 neuronal activity encodes movement kinematics, not movement dynamics. Exp Brain Res. 80:351–364.
Kennedy C, Sakurada O, Shinohara M, Jehle J, Sokoloff L. 1978. Local cerebral glucose utilization in the normal conscious macaque monkey. Ann Neurol. 4:293–301.
Kilner JM, Friston KJ, Frith CD. 2007. The mirror-neuron system: a Bayesian perspective. Neuroreport. 18:619–623.
Kilner JM, Vargas C, Duval S, Blakemore SJ, Sirigu A. 2004. Motor activation prior to observation of a predicted movement. Nat Neurosci. 7:1299–1301.
Kobayashi Y, Amaral DG. 2003. Macaque monkey retrosplenial cortex: II. Cortical afferents. J Comp Neurol. 466:48–79.
Lewis JW, Van Essen DC. 2000a. Corticocortical connections of visual, sensorimotor, and multimodal processing area in the parietal lobe of the macaque monkey. J Comp Neurol. 428:112–137.
Lewis JW, Van Essen DC. 2000b. Mapping of architectonic subdivisions in the macaque monkey, with emphasis on parieto-occipital cortex. J Comp Neurol. 428:79–111.
Luppino G, Hamed SB, Gamberini M, Matelli M, Galletti C. 2005. Occipital (V6) and parietal (V6A) areas in the anterior wall of the parieto-occipital sulcus of the macaque: a cytoarchitectonic study. Eur J Neurosci. 21:3056–3076.

Luppino G, Murata A, Govoni P, Matelli M. 1999. Largely segregated parietofrontal connections linking rostral intraparietal cortex (areas AIP and VIP) and the ventral premotor cortex (areas F5 and F4). Exp Brain Res. 128:181–187.

Marconi B, Genovesio A, Battaglia-Mayer A, Ferraina S, Squatrito S, Molinari M, Laquaniti F, Caminiti R. 2001. Eye-hand coordination during reaching. I. Anatomical relationships between parietal and frontal cortex. Cereb Cortex. 11:513–527.

Matelli M, Camarda R, Glickstein M, Rizzolatti G. 1986. Afferent and efferent projections of the inferior area 6 in the macaque monkey. J Comp Neurol. 251:281–298.

Matelli M, Govoni P, Galletti C, Kutz DF, Luppino G. 1998. Superior area 6 afferents from the superior parietal lobule in the macaque monkey. J Comp Neurol. 402:327–352.

Medalla M, Barbas H. 2006. Diversity of laminar connections linking periarcuate and lateral intraparietal areas depends on cortical structure. Eur J Neurosci. 23:161–179.

Morecraft RJ, Cipolloni PB, Stilwell-Morecraft KS, Gedney MT, Pandya DN. 2004. Cytoarchitecture and cortical connections of the posterior cingulate and adjacent somatosensory fields in the rhesus monkey. J Comp Neurol. 469:37–69.

Morris R, Petrides M, Pandya DN. 1999. Architecture and connections of retrosplenial area 30 in the rhesus monkey (Macaca mulatta). Eur J Neurosci. 11:2506–2518.

Mountcastle VB, Lynch JC, Georgopoulos AP, Sakata H, Acuna C. 1975. Posterior parietal association cortex of the monkey: command function for operations within extrapersonal space. J Neurophysiol. 38:871–908.

Murata A, Gallese V, Luppino G, Kaseda M, Sakata H. 2000. Selectivity for the shape, size, and orientation of objects for grasping in neurons of monkey parietal area AIP. J Neurophysiol. 83:2580–2601.

Nakamura H, Kuroba T, Wakita M, Kusunoki M, Kato A, Mikami A, Sakata H, Itoh K. 2001. From three-dimensional space vision to prehensile hand movements: the lateral intraparietal area links the area V3A and the anterior intraparietal area in macaques. J Neurosci. 21:8174–8187.

Nelson RJ, Sur M, Fellman DJ, Kaas JH. 1980. Representations of the body surface in postcentral parietal cortex of *Macaca fascicularis*. J Comp Neurol. 192:611–643.

Olson CR, Musil SY, Goldberg ME. 1996. Single neurons in posterior cingulate cortex of behaving macaque: eye movement signals. J Neurophysiol. 76:3285–3300.

Pandya DN, Seltzer B. 1982. Intrinsic connections and architectonics of posterior parietal cortex in the rhesus monkey. J Comp Neurol. 204:196–210.

Pearson RCA, Powell TPS. 1985. The projection of the primary somatic sensory cortex upon area 5 in the monkey. Brain Res Rev. 9:89–107.

Petrides M. 1995. Impairments on nonspatial self-ordered working memory tasks after lesions of the mid-dorsal part of the lateral frontal cortex in the monkey. J Neurosci. 15:359–375.

Petrides M, Alivisatos B, Evans AC, Meyer E. 1993. Dissociation of human mid-dorsolateral from posterior dorsolateral frontal cortex in memory processing. Proc Natl Acad Sci USA. 90:873–877.

Petrides M, Pandya DN. 1984. Projections to the frontal cortex from the posterior parietal region in the rhesus monkey. J Comp Neurol. 228:105–116.

Pons TP, Garraghty PE, Cusick CG, Kaas JH. 1985. The somatotopic organization of area 2 in macaque monkeys. J Comp Neurol. 241:445–466.

Raos V, Evangeliou MN, Savaki HE. 2004. Observation of action: grasping with the mind's hand. Neuroimage. 23:193–201.

Raos V, Evangeliou MN, Savaki HE. 2007. Mental simulation of action in the service of action perception. J Neurosci. 27:12675–12683.

Rizzolatti G, Fadiga L, Gallese V, Fogassi L. 1996. Premotor cortex and the recognition of motor actions. Cogn Brain Res. 3:131–141.

Rozzi S, Calzavara R, Belmalih A, Borra E, Gregoriou GG, Matelli M, Luppino G. 2005. Cortical connections of the inferior parietal cortical convexity of the macaque monkey. Cereb Cortex. 16:1389–1417.

Ruby P, Decety J. 2001. Effect of subjective perspective taking during simulation of action: a PET investigation of agency. Nat Neurosci. 4:546–550.

Saito DN, Okada T, Morita Y, Yonekura Y, Sadato N. 2003. Tactile-visual cross-modal shape matching: a functional MRI study. Brain Res Cogn Brain Res. 17:14–25.

Sakata H, Taira M, Murata A, Mine S. 1995. Neural mechanisms of visual guidance of hand action in the parietal cortex of the monkey. Cereb Cortex. 5:429–438.

Savaki HE, Dalezios Y. 1999. ^{14}C-Deoxyglucose mapping of the monkey brain during reaching to visual targets. Prog Neurobiol. 58:479–540.

Savaki HE, Kennedy C, Sokoloff L, Mishkin M. 1993. Visually guided reaching with the forelimb contralateral to a "blind" hemisphere: a metabolic mapping study in monkeys. J Neurosci. 13:2772–2789.

Savaki HE, Raos VC, Dalezios Y. 1997. Spatial cortical patterns of metabolic activity in monkeys performing a visually guided reaching task with one forelimb. Neuroscience. 76:1007–1034.

Shipp S, Blanton M, Zeki S. 1998. A visuo-somatomotor pathway through superior parietal cortex in the macaque monkey: cortical connections of areas V6 and V6A. Eur J Neurosci. 10:3171–3193.

Shmuelof L, Zohary E. 2006. A mirror representation of others' actions in the human anterior parietal cortex. J Neurosci. 26:9736–9742.

Sirigu A, Daprati E, Ciancia S, Giraux P, Nighoghossian N, Posada A, Haggard P. 2004. Altered awareness of voluntary action after damage to the parietal cortex. Nat Neurosci. 7:80–84.

Sirigu A, Daprati E, Pradat-Diehl P, Franck N, Jeannerod M. 1999. Perception of self-generated movement following left parietal lesion. Brain. 122(Pt 10):1867–1874.

Sirigu A, Duhamel JR, Cohen L, Pillon B, Dubois B, Agid Y. 1996. The mental representation of hand movements after parietal cortex damage. Science. 273:1564–1568.

Sokoloff L, Reivich M, Kennedy C, Des Rosiers MH, Patlak CS, Pettigrew KS, Sakurada O, Shinohara M. 1977. The [^{14}C]-deoxyglucose method for the measurement of local cerebral glucose utilization: theory, procedure, and normal values in the conscious and anesthetized albino rat. J Neurochem. 28:879–916.

Tsutsui K, Jiang M, Sakata H, Taira M. 2003. Short-term memory and perceptual decision for three-dimensional visual features in the caudal intraparietal sulcus (area CIP). J Neurosci. 23:5486–5495.

Vanduffel W, Fize D, Mandeville JB, Nelissen K, Van Hecke P, Rosen BR, Tootell RB, Orban GA. 2001. Visual motion processing investigated using contrast agent-enhanced fMRI in awake behaving monkeys. Neuron. 32:565–577.